Molecular Biology of the Cell
Vol. 8, 2307–2327, November 1997

A Novel RING Finger Protein Complex Essential for a Late Step in Protein Transport to the Yeast Vacuole

Stephanie E. Rieder and Scott D. Emr*

Department of Biology, Division of Cellular and Molecular Medicine, Howard Hughes Medical Institute, University of California, San Diego, School of Medicine, La Jolla, California 92093-0668

Submitted June 4, 1997; Accepted August 27, 1997
Monitoring Editor: Ari Helenius

Protein transport to the lysosome-like vacuole in yeast is mediated by multiple pathways, including the biosynthetic routes for vacuolar hydrolases, the endocytic pathway, and autophagy. Among the more than 40 genes required for vacuolar protein sorting (*VPS*) in *Saccharomyces cerevisiae*, mutations in the four class C *VPS* genes result in the most severe vacuolar protein sorting and morphology defects. Herein, we provide complementary genetic and biochemical evidence that the class C *VPS* gene products (Vps18p, Vps11p, Vps16p, and Vps33p) physically and functionally interact to mediate a late step in protein transport to the vacuole. Chemical cross-linking experiments demonstrated that Vps11p and Vps18p, which both contain RING finger zinc-binding domains, are components of a hetero-oligomeric protein complex that includes Vps16p and the Sec1p homologue Vps33p. The class C Vps protein complex colocalized with vacuolar membranes and a distinct dense membrane fraction. Analysis of cells harboring a temperature-conditional *vps18* allele ($vps18^{tsf}$) indicated that Vps18p function is required for the biosynthetic, endocytic, and autophagic protein transport pathways to the vacuole. In addition, $vps18^{tsf}$ cells accumulated multivesicular bodies, autophagosomes, and other membrane compartments that appear to represent blocked transport intermediates. Overproduction of either Vps16p or the vacuolar syntaxin homologue Vam3p suppressed defects associated with $vps18^{tsf}$ mutant cells, indicating that the class C Vps proteins and Vam3p may functionally interact. Thus we propose that the class C Vps proteins are components of a hetero-oligomeric protein complex that mediates the delivery of multiple transport intermediates to the vacuole.

INTRODUCTION

The intracellular organelles in eukaryotic cells have distinct biochemical and morphological characteristics defined by their unique protein and lipid compositions. Thus, specific transport systems are required to accurately deliver protein and membrane components to their correct intracellular locations. Biochemical and genetic studies have identified a large number of well-conserved proteins required for this process, including members of protein families that perform analogous functions at different transport steps. For example, members of the syntaxin and synaptobrevin families (SNAREs) contribute to transport specificity by mediating interactions between transport intermediates and their appropriate target membranes (see Rothman, 1994; Hanson *et al.*, 1997). Other proteins that regulate docking and fusion events include the NSF/Sec18p ATPase, the Rab/Ypt family of GTPases, and the Sec1 protein family (see Pfeffer, 1996; Hay and Scheller, 1997; Novick and Zerial, 1997). In addition, specialized accessory factors are required at individual transport steps, such as the macromolecular "Exocyst" protein complex that mediates Golgi-to-plasma membrane transport in yeast (TerBush *et al.*, 1996).

The mammalian lysosome and the functionally analogous vacuole in *Saccharomyces cerevisiae* are acidic organelles that play an important role in macromolecular degradation, metabolite storage, and ion homeostasis (reviewed in Kornfeld and Mellman, 1989;

* Corresponding author.

Klionsky *et al.*, 1990). Protein and membrane transport to the vacuole is mediated by multiple pathways, including 1) the biosynthetic routes for newly synthesized vacuolar hydrolases, originating in the early secretory pathway; 2) the endocytic pathway, originating at the plasma membrane; and 3) autophagy, originating in the cytoplasm.

As in mammalian cells, most vacuolar hydrolases are synthesized as inactive precursors that transit through the secretory pathway until they reach the late Golgi, where they are sorted away from the proteins destined for secretion and targeted for delivery to the vacuole (reviewed in Horazdovsky *et al.*, 1995; Stack *et al.*, 1995; Traub and Kornfeld, 1997). Several studies indicate that at least two pathways mediate biosynthetic transport between the late Golgi and the vacuole. Vacuolar hydrolases such as carboxypeptidase Y (CPY)[1] and carboxypeptidase S (CPS) are delivered to the vacuole via an endosome-like compartment, but alkaline phosphatase (ALP) transits to the vacuole in transport intermediates that appear to bypass the prevacuolar endosome (see Horazdovsky *et al.*, 1995; Stack *et al.*, 1995; Cowles *et al.*, 1997).

Cell surface components destined for endocytosis and degradation, including certain receptors and their ligands, are internalized and delivered to the vacuole/lysosome by the endocytic pathway (reviewed in Gruenberg and Maxfield, 1995; Seaman *et al.*, 1996). Although some internalized components are recycled back to the plasma membrane from an early endosomal compartment, cell surface components destined for degradation continue on to a late endosomal compartment prior to reaching the vacuole/lysosome. As in mammalian cells, the yeast endocytic pathway appears to merge with the biosynthetic pathway at a prevacuolar endosome-like compartment and subsequently their distinct cargo transit together to the vacuole (Singer and Riezman, 1990; Vida *et al.*, 1993; Piper *et al.*, 1995; Rieder *et al.*, 1996; Babst *et al.*, 1997).

Autophagy mediates the bulk transport of cytosolic components to the vacuole/lysosome, a process that is enhanced under starvation conditions (see Takeshige *et al.*, 1992; Dunn, 1993). During starvation-induced autophagy in yeast, double-membrane autophagosomes form in the cytoplasm and fuse with the vacuolar membrane, thereby delivering single-membrane autophagic bodies into the vacuolar lumen where they are rapidly degraded (Takeshige *et al.*, 1992; Baba *et al.*, 1994). In addition, a constitutive autophagic pathway mediates the delivery of aminopeptidase I (API) from the cytoplasm to the vacuole (Harding *et al.*, 1996; Scott *et al.*, 1996; Klionsky, 1997).

To identify the transport components involved in the delivery of proteins to the vacuole, genetic selections in *S. cerevisiae* were used isolate mutants that missort and secrete the vacuolar hydrolase CPY (Bankaitis *et al.*, 1986; Rothman and Stevens, 1986; Robinson *et al.*, 1988; Rothman *et al.*, 1989). Many of the resulting vacuolar protein sorting (*vps*) mutants were also isolated with screens for vacuolar peptidase deficiencies (*pep*; Jones, 1977) and vacuolar morphology defects (*vam*; Wada *et al.*, 1992). Together, these mutants define more than 40 complementation groups and have been categorized into six classes (A–F) with respect to their vacuolar protein sorting, morphology, and acidification defects (Banta *et al.*, 1988; Raymond *et al.*, 1992). The four class C *vps* mutants (*vps18/pep3, vps16*, *vps11/end1/pep5*, and *vps33/slp1*) exhibit the most severe vacuolar protein sorting and morphology defects. These mutants lack any structure resembling a normal vacuole and instead accumulate small vesicles and other aberrant membrane compartments (Banta *et al.*, 1988; Woolford *et al.*, 1990; Preston *et al.*, 1991). In addition, the class C *vps* mutants exhibit multiple defects consistent with the absence of vacuoles, including temperature-sensitive growth defects, osmotic sensitivity, calcium sensitivity, reduced amino acid pools, and sporulation defects (Banta *et al.*, 1988; Robinson *et al.*, 1988; Dulic and Riezman, 1989; Wada *et al.*, 1990; Woolford *et al.*, 1990; Preston *et al.*, 1991).

Each of the four class C *VPS* genes has been cloned. *VPS33/SLP1* encodes a Sec1p homologue of 691 amino acids (Banta *et al.*, 1990; Wada *et al.*, 1990). Sec1 protein family members are thought to enhance transport specificity by regulating interactions between members of the synaptobrevin and syntaxin protein families (Hata *et al.*, 1993; Garcia *et al.*, 1994; Pevsner *et al.*, 1994; Garcia *et al.*, 1995; Hata and Sudhof, 1995). *VPS16* encodes a 798-amino acid protein that lacks homology to characterized proteins or protein motifs (Horazdovsky and Emr, 1993). *VPS18/PEP3* and *VPS11/END1/PEP5* encode hydrophillic proteins of 918 and 1029 amino acids, respectively (Dulic and Riezman, 1989; Woolford *et al.*, 1990; Preston *et al.*, 1991; Robinson *et al.*, 1991), both of which contain C-terminal RING finger zinc-binding domains. The RING finger domain is important for the biological activity of the *VPS18/PEP3* gene product, because *vps18* cells harboring a mutation in this domain exhibit temperature-conditional CPY sorting defects (Robinson *et al.*, 1991). The *VPS18/PEP3* gene product shares significant homology with the *Drosophila melanogaster* dor protein, which also has a C-terminal RING finger domain (Shestopal *et al.*, 1997). The *dor* locus was first identified in mutant flies with deep orange (dor) eyes that exhibit multiple pigment deposition defects (see Lindsley and Zimm, 1992). For clarity, the class C *VPS*

[1] Abbreviations used: ALP, alkaline phosphatase; API, aminopeptidase I; CPS, carboxypeptidase S; CPY, carboxypeptidase Y; DSP, dithiobis(succinimidyl-propionate); FM4–64, [*N*-(3-triethylammoniumpropyl)-4-(*p*-diethylaminophenylhexatrienyl)pyridinum dibromide]; PrA, proteinase A; PrB, proteinase B; TCA, trichloroacetic acid.

Table 1. *S. cerevisiae* strains used in this study

Strain	Genotype	Reference or source
SEY6210	*MATα leu2-3,112 ura3-52 his3-Δ200 trp1-Δ901 lys2-801 suc2-Δ9*	Robinson *et al*. (1988)
SEY6211	*MAT***a** *leu2-3,112 ura3-52 his3-Δ200 trp1-Δ901 ade2-101 suc2-Δ9*	Robinson *et al*. (1988)
SEY6210.1	SEY6210; *MAT***a**	Babst *et al*. (1997)
TVY1	SEY6210; *pep4Δ::LEU2*	Thomas Vida
SRY18T-1	SEY6210; *vps18^{tsf}-1*	This study
SRY18T-4	SRY18T-1; *MAT***a**	This study
SRY18T-9	SRY18T-1; *pep4Δ::LEU2*	This study
SEY33-4	SEY6210; *vps33-4*	Robinson *et al*. (1988); Banta *et al*. (1990)
SEY6211*e*	SEY6211; *vps11-Δ2::LEU2*	Dulic and Riezman (1989)
JSR18Δ1	SEY6210; *vps18-Δ1::TRP1*	Robinson *et al*. (1991)
LBY317	SEY6210; *vps33-Δ2::HIS3*	Banta *et al*. (1990)
BHY113	SEY6210; *vps16-Δ2::HIS3*	Horazdovsky and Emr (1993)

genes will be referred to as *VPS18*, *VPS11*, *VPS16*, and *VPS33* in this report.

Herein we present genetic and biochemical evidence for direct physical and functional interactions between the class C Vps proteins. In addition, analysis of a temperature-conditional *vps18* allele indicated that Vps18p function is required for the biosynthetic, endocytic, and autophagic protein transport pathways to the vacuole. On the basis of these and other results, we propose that the class C Vps proteins function together in a multiprotein complex to mediate the docking and/or fusion of late transport intermediates with the vacuole.

MATERIALS AND METHODS

Strains, Media, and Materials

The *S. cerevisiae* strains used in these studies are listed in Table 1. Yeast strains were grown in standard yeast extract-peptone-dextrose (YPD) or synthetic medium with dextrose (SD) supplemented as needed with amino acids (Sherman *et al*., 1979). To examine starvation-induced autophagy, yeast strains were incubated in nitrogen-deficient medium (SD-N; synthetic medium without amino acids and ammonium sulfate plus 2% dextrose). The *Escherichia coli* strain used in this study was XL1-Blue [*supE44 thi-1 lac endA1 gyrA96 hsdR17 relA1* (*F′ proAB lac1q ZΔM15 Tn10*)]. Bacterial strains were grown on standard media (Miller, 1972), supplemented with 75 μg/ml ampicillin for plasmid retention. Materials were purchased from Fisher Scientific (Fairlane, NJ) or Sigma (St. Louis, MO) unless otherwise indicated.

Plasmid Constructions

Standard recombinant DNA techniques were performed as previously described (Maniatis *et al*., 1982) by using reagents from Boehringer Mannheim Biochemicals (Indianapolis, IN) or New England Bioloabs (Beverly, MA). The integrative plasmid pSRY18T-406 carrying the *vps18^{tsf}-1* (C_{826}S) allele was generated by inserting the *Kpn*I–*Pvu*II fragment of pJSR9 into the *Kpn*I and *Sma*I sites of pRS406 (Sikorski and Hieter, 1989). Plasmid pVAM3.426 (2μ*VAM3*) was constructed by subcloning the *Bst*BI–*Nsi*I fragment of p351R1 (Wada *et al*., 1997) into pRS426 (Sikorski and Hieter, 1989). Plasmid pJR18–5 (2μ*VPS18*) was constructed by subcloning the *Kpn*I–*Sac*I fragment from pJSR6 into pPHY16. Plasmid pSEY8-VPS11 (2μ*VPS11*) was constructed by subcloning the *Bgl*II–*Hin*dIII fragment including the *VPS11* gene into pSEY8. An in-frame gene fusion between the *E. coli trpE* and *VPS18* genes was constructed by subcloning the *Xba*I–*Eco*RV fragment of *VPS18* into the blunted *Xba*I–*Hin*dIII sites of pATH2 (Dieckmann and Tzagoloff, 1985), generating pKK18-FUS. An in-frame *trpE-VPS11* gene fusion was generated by fusing the *Eco*RI–*Xba*I fragment of *VPS11* to the *trpE* gene in pATH3 (Dieckmann and Tzagoloff, 1985), generating pTrpE-VPS11. Plasmids pVPS16–36 (2μ*VPS16*), pLB33–162 (2μ*VPS33*), pJSR6 (*CEN VPS18*), pLB33–21 (*CEN VPS33*), pJSR9 [*CEN vps18^{tsf}-1* (C_{826}S)] have been previously described (Banta *et al*., 1990; Robinson *et al*., 1991; Horazdovsky and Emr, 1993). Plasmid pDB192 (2μ*STE6*) was a generous gift from David Bedwell (University of Alabama, Birmingham, AL).

Yeast and Bacterial Methods

Standard yeast and *E. coli* genetic techniques were carried out as described previously (Miller, 1972; Sherman *et al*., 1979). Yeast transformations were performed with the lithium acetate method (Ito *et al*., 1983) using single-stranded DNA as carrier (Schiestl and Gietz, 1989). *E. coli* transformations were done according to the method of Hanahan (1983). The chromosomal *vps18^{tsf}-1* (C_{826}S) mutant strain, SRY18T-1, was generated using the "pop-in/pop-out" allele replacement technique described by Rothstein (1991). Plasmid pSRY18T-406 [*vps18^{tsf}-1* (C_{826}S), *URA3*] was linearized with *Bal*I and transformed into SEY6210 cells. Ura$^+$ transformants, harboring the *URA3* gene flanked by the *VPS18* and *vps18^{tsf}-1* genes if the construct correctly integrated at the *VPS18* locus, were streaked onto plates with 5-fluoroorotic acid (PCR, Gainesville, FL) to select for excision of the plasmid. The resulting colonies were tested for the *vps18^{tsf}* phenotype to identify strains with the *vps18^{tsf}-1* (C_{826}S) allele. To disrupt the *PEP4* gene in SRY18T-1, plasmid pP1::LEU2 (Ammerer *et al*., 1986) was digested with *Bam*HI and transformed into SRY18T-1. The disruption of *PEP4* was confirmed in Leu$^+$ transformants by the loss of the proteinase A (PrA) protein and its activity, yielding strain SRY18T-4 (*vps18^{tsf}-1 pep4Δ*). The strain SRY18T-4 (*vps18^{tsf}-1; MAT***a**) was generated from SRY18T-1 (*vps18^{tsf}-1, MATα*) with the *HO* gene as described by Herskowitz and Jensen (1991).

Fluorescence and Electron Microscopy

Fluorescence Microscopy. FM4–64 [*N*-(3-triethylammoniumpropyl)-4-(*p*-diethylaminophenyl-hexatrienyl)pyridinum dibromide; Molecular Probes, OR] was used to examine the endocytic pathway and vacuolar morphology using methods similar to those described by Vida and Emr (1995). Yeast cell cultures were grown at 26°C in

YPD to midlogarithmic phase (OD_{600} of 0.4–0.8 per ml). Prior to staining, the cultures were split and incubated for 15 min at either 26°C or 38°C. The cells were stained with 32 μM FM4–64 for 15 min, harvested, and chased in prewarmed YPD for 45 min (26°C) or 30 min (38°C).

Electron Microscopy. To examine starvation-induced autophagy, yeast strains were grown to midlogarithmic phase in YPD at 26°C and then were harvested, washed, and resuspended in nitrogen-starvation medium (SD-N). The cells were incubated in SD-N for 2.5 h at either 26°C or 38°C, fixed, and prepared for electron microscopy using the osmium/thiocarbohydrazide-based technique previously described (Banta *et al.*, 1988; Rieder *et al.*, 1996). To examine cell morphology, the SRY18T-1, SEY6210, and JRY18Δ1 strains were grown to midlogarithmic phase in YPD at 26°C. The SRY18T-1 (*vps18^{tsf}-1*) and SEY6210 (WT) cultures were then split and incubated further at 26°C or were shifted to 38°C for 2.5 h. The cells were harvested and prepared for electron microscopy as previously described (Rieder *et al.*, 1996), except that the time of cell wall digestion was reduced to 1 h.

Cell Labeling and Immunoprecipitation

Yeast cells were labeled as described previously (Rieder *et al.*, 1996). Cells were grown to midlogarithmic phase in SD medium supplemented with amino acids. Whole cells were labeled with Expres^{35}S (New England Nuclear, Boston, MA) at 2–5 OD_{600} U/ml in SD medium containing amino acids, 100 μg/ml α_2-macroglobulin, and 500 μg/ml bovine serum albumin to stabilize secreted proteins. The chase was initiated by the addition of methionine, cysteine, yeast extract, and glucose (final concentrations of 5 mM, 1 mM, 0.2%, and 4%, respectively). Spheroplasts were generated by incubating cells with zymolyase-100T (Seikagaku Kogyo, Tokyo) to remove the cell wall as described previously (Rieder *et al.*, 1996). Spheroplasts were ^{35}S-labeled as above, except the labeling medium and the chase solution included sorbitol (1 M, final concentration). The pulse–chase reactions were stopped by adding the energy poisons sodium azide and NaF, each to a final concentration of 20 mM.

Proteins were precipitated by addition of trichloroacetic acid (TCA) to a final concentration of 8–10% and subjected to immunoprecipitation as described previously (Cereghino *et al.*, 1995), except that urea cracking buffer (50 mM Tris(hydroxymethyl)aminomethane hydrochloride, pH 7.2, 6 M urea, 1% SDS) was used to resuspend the dried TCA pellets prior to glass bead lysis and protein solubilization. Samples subjected to sequential immunoprecipitations were dissociated from the first antibody by heating to 70°C for 10 to 15 min in 50 μl of urea cracking buffer, diluted in 1 ml of Tween-20 buffer, and subjected to a second immunoprecipitation. Prior to SDS-PAGE, CPS immunoprecipitates were treated with endoglycosidase H (Cowles *et al.*, 1997) to collapse the differentially glycosylated forms of CPS into single pro-CPS and m-CPS bands (Spormann *et al.*, 1991).

Polyclonal antisera against Vps18p and Vps11p were raised against TrpE-Vps18 and TrpE-Vps11 fusion proteins that were produced in XL1-Blue *E. coli* cells harboring pKK18-FUS or pTrpE-Vps11, respectively. The fusion proteins were purified and used to immunize New Zealand White rabbits as described previously (Horazdovsky and Emr, 1993). Polyclonal antisera against CPY, ALP, Vps33p, Vps16p, Vps10p, Pep12p, and CPS have been previously described (Robinson *et al.*, 1988; Klionsky and Emr, 1989; Banta *et al.*, 1990; Horazdovsky and Emr, 1993; Marcusson *et al.*, 1994; Becherer *et al.*, 1996; Cowles *et al.*, 1997). Antisera recognizing Kex2p, Ste6p, and API were generous gifts from Robert Fuller (University of Michigan, Ann Arbor, MI), David Bedwell (University of Alabama, Birmingham, AL), and Dan Klionsky (University of California, Davis.

Differential Centrifugation Experiments

^{35}S-labeled spheroplasts were prepared as described above and were resuspended in ice-cold lysis buffer [200 mM sorbitol, 50 mM potassium acetate, 1 mM EDTA, 20 mM *N*-(2-hydroxyethyl)piperazine-*N*′-(2-ethanesulfonic acid), pH adjusted to 6.8 with KOH] containing protease inhibitors (20 μg/ml phenylmethylsulfonyl fluoride, 5 μg/ml antipain, 1 μg/ml aprotinin, 1 μg/ml leupeptin, 1 μg/ml pepstatin, 10 μg/ml α_2-macroglobulin), except buffer T [Tris(hydroxymethyl)aminomethane, pH 6.8 and 1 mM EDTA] was used for Figure 2A. The cell suspension was homogenized in a Dounce homogenizer ~10 times in an ice-cold glass tissue homogenizer and the resulting crude lysate was centrifuged at 300 × *g* for 5 min to remove unlysed spheroplasts. For differential centrifugation experiments, the cleared lysate was centrifuged at 13,000 × *g* for 15 min to generate the P13 pellet; the remaining supernatant fraction (S13) was centrifuged at 100,000 × *g* for 45 min to generate the P100 pellet and S100 supernatant fractions. To investigate protein interactions with pelletable cell components, the cleared lysate was adjusted to 6 M urea, 1 M NaCl, 1% Triton X-100, and 0.1 M Na_2CO_3, pH 11. After 15 min on ice, the samples were centrifuged at 100,000 × *g* for 45 min. The proteins in each fraction were precipitated the addition of TCA and were processed for immunoprecipitation.

Density Gradient Analysis

For Accudenz density gradients, Accudenz (Accurate Chemical and Scientific, Westbury, NY) solutions were prepared (as percent, wt/vol) in lysis buffer with protease inhibitors. The step gradients consisted of 1.25-ml of 37% Accudenz, 1.5-ml steps of 30%, 27%, 23%, and 20% Accudenz, and 1-ml steps of 17%, 13%, and 9% Accudenz. From 15 to 25 OD_{600} U of ^{35}S-labeled spheroplasts were lysed as described above and cleared of unbroken cells by centrifuging at 300 × *g* for 5 min. The resulting lysate was loaded on top of the gradients and were then centrifuged in a Beckman SW41 rotor at 170,000 × *g* for 16 to 18 h at 4°C. Fractions were collected form the top and the proteins were precipitated with TCA. The distribution of ^{35}S-labeled proteins was analyzed by immunoprecipitation, SDS-PAGE, and fluorography. Unlabeled ALP was detected by Western blot and ECL analysis as described by Babst *et al.* (1997) using ALP-specific monoclonal antibodies (Molecular Probes). Floatation experiments were completed as above, except that the samples were mixed with an Accudenz solution (40% final concentration) and loaded at the bottom of the density gradients. Protein recovery was quantified by using a Molecular Dynamics PhosphorImager (Sunnyvale, CA) or densitometry (NIH Image software).

Cross-Linking of Cell Extracts

Cells were converted to spheroplasts, ^{35}S-labeled, and chased as described above. The spheroplasts were lysed at 5–10 OD_{600} U/ml in cross-linking buffer (0.1 M KH_2PO_4, pH 7.5, 1 mM EDTA) with protease inhibitors. The cross-linker DSP [dithiobis(succinimidyl-propionate); Pierce, Rockford, IL], dissolved in dimethyl sulfoxide, was added to the lysates at a final concentration of 200 μg/ml. Mock-treated control samples received dimethyl sulfoxide alone. The extracts were incubated at 23°C for 30 min, after which the reaction was quenched by the addition of hydroxylamine to a final concentration of 20 mM. Proteins were precipitated by the addition of TCA and processed for immunoprecipitation using Vps11p- or Vps18p-specific antiserum (under denaturing but nonreducing conditions). The first antibody was irreversibly denatured and the immunoprecipitates were eluted by heating for 15 min in urea cracking buffer (with or without 1% 2-mercaptoethanol). The eluted primary immunoprecipitates were then subjected to reimmunoprecipitation with the appropriate antisera. The final immunoprecipitates were reduced with 2-mercaptoethanol prior to SDS-PAGE.

RESULTS

The vps18^{tsf} RING Finger Mutant Exhibits Temperature-Conditional Defects in the Transport of Multiple Vacuolar Proteins

Mutations in the class C *VPS* genes (*VPS18*, *VPS11*, *VPS33*, and *VPS16*) result in a common set of severe vacuolar protein sorting and morphology defects (see INTRODUCTION), suggesting that the class C *VPS* gene products may function at a common step in the vacuolar protein transport pathway. Sequence analysis indicated that each of the four class C *VPS* gene products (Vps18p, Vps11p, Vps16p, and Vps33p) has one or more regions predicted to form α-helical coiled-coil domains (Figure 1A; Lupas *et al.*, 1991) that may mediate protein–protein interactions (see Lupus, 1996). In addition, recent examination of the Vps18p and Vps11p protein sequences revealed that they both contain C-terminal cysteine-rich regions that conform to the RING finger zinc-binding motif (Figure 1A). RING finger domains have the consensus sequence of $CX_2CX_{9-39}CX_{1-3}HX_{2-3}CX_2CX_{4-48}CX_2C$ (C3HC4) and bind two Zn^{2+} ions in a unique "cross-brace" structure (Figure 1B; see Borden and Freemont, 1996; Saurin *et al.*, 1996). Vps18p and Vps11p contain the H2 RING finger variant, where the fourth cysteine is replaced by a histidine residue (C3H2C3; Figure 1B). RING finger zinc-binding domains are found in a large family of diverse proteins and may mediate protein–protein interactions (Borden and Freemont, 1996; Saurin *et al.*, 1996).

The RING finger domain is important for the biological function of Vps18p. Robinson *et al.* (1991) dem-

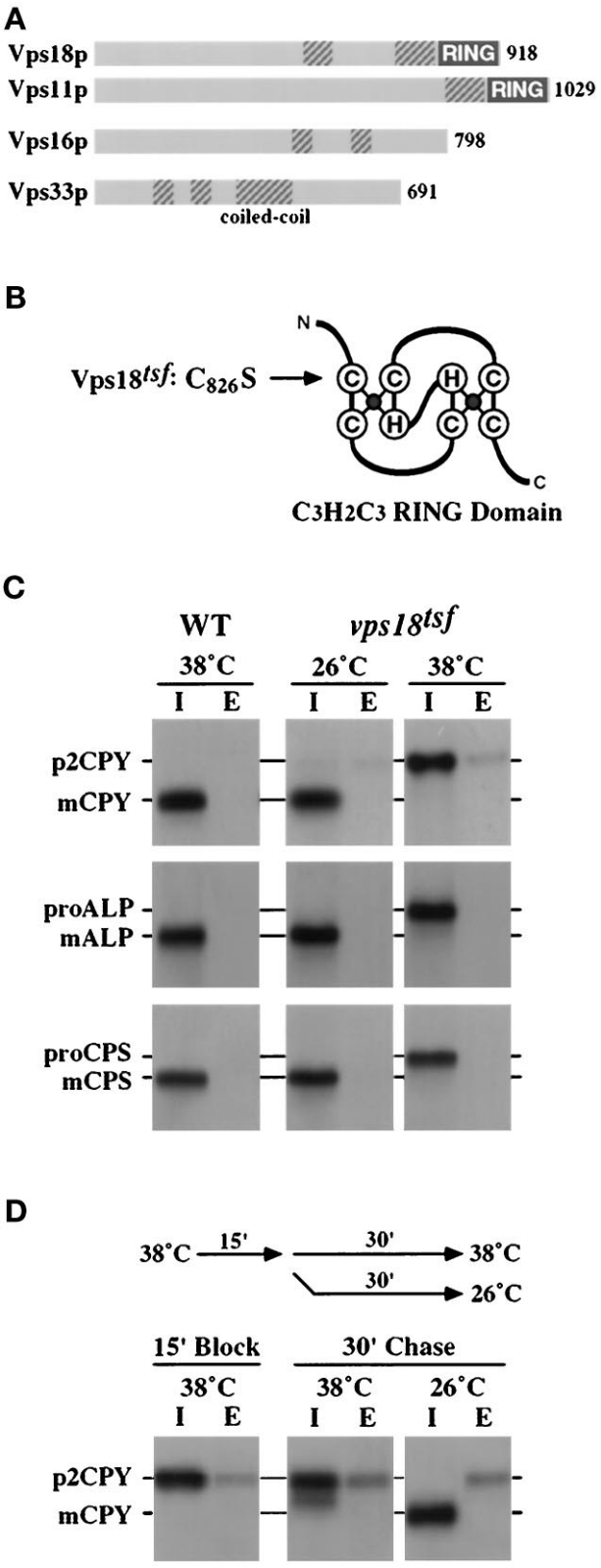

Figure 1.

Figure 1. *vps18^{tsf}* RING finger mutant exhibits rapid temperature-conditional defects in the transport of multiple vacuolar proteins. (A) Schematic summary of the four class C Vps proteins: Vps18, Vps11p, Vps16p and the Sec1p homologue Vps33. Vps18p and Vps11p both have C-terminal RING finger zinc-binding domains (RING). Domains predicted to adopt an α-helical coiled-coil confirmation (COILS 2.1, Lupas *et al.*, 1991) are indicated with hatched boxes. (B) Schematic diagram of the RING finger zinc-binding domain (adapted from Borden and Freemont, 1996). Mutation of the first conserved cysteine in the RING finger domain of Vps18p ($C_{826}S$) renders Vps18p temperature-sensitive for function (Vps18^{tsf}p). (C) WT (wild-type, SEY6210) and *vps18^{tsf}* (SRY18T-1) spheroplasts were preincubated for 5 min at 26°C or 38°C prior to labeling with Expres^{35}S for 15 min and chasing for 45 min. The labeled cultures were separated into intracellular (I) and extracellular (E) fractions. The abundance and sizes of CPY, ALP, and CPS in these fractions were determined by immunoprecipitation, SDS-PAGE, and fluorography. The Golgi-modified precursor (p2, pro) and mature (m) forms of the vacuolar proteins are indicated. (D) *vps18^{tsf}* (SRY18T-1) spheroplasts were preincubated for 5 min at 38°C prior to labeling with Expres^{35}S for 10 min and chasing for 15 min. The cultures were then split, chased for an additional 30 min at either 38°C or 26°C, and then separated into intracellular (I) and extracellular (E) fractions. The abundance and sizes of CPY in these fractions were determined by immunoprecipitation, SDS-PAGE, and fluorography.

onstrated that mutation of the first conserved cysteine of the RING finger domain ($C_{826}S$; Figure 1B) results in a temperature-conditional defect in CPY processing. To further use this temperature-sensitive for function (*tsf*) *vps18* allele ($C_{826}S$; *vps18^{tsf}-1*) and characterize the immediate consequences of loss of Vps18p activity, the chromosomal wild-type *VPS18* locus was replaced with the *vps18^{tsf}-1* mutant allele in SEY6210 cells. The resulting strain, SRY18T-1 (referred to hereafter as *vps18^{tsf}*) was used in this report to explore genetic interactions with *VPS18* and to examine the role of Vps18p in protein transport along the biosynthetic, endocytic, and autophagic pathways to the vacuole (Figure 1, see Figures 2–6).

Newly synthesized vacuolar hydrolases traffic from the late Golgi to the vacuole by at least two different biosynthetic pathways. The soluble vacuolar hydrolases CPY, PrA, and proteinase B (PrB) and integral membrane protein CPS appear to transit to the vacuole via an endosomal intermediate compartment, but ALP, another integral membrane protein, follows an alternative route to the vacuole in transport intermediates that appear to bypass the endosome (reviewed in Horazdovsky *et al.*, 1995; Stack *et al.*, 1995; Cowles *et al.*, 1997). To analyze the direct requirement for Vps18p function in protein transport along both the CPY/CPS and ALP biosynthetic pathways, the fate of multiple newly synthesized vacuolar hydrolases was examined in *vps18^{tsf}* cells at either permissive (26°C) or nonpermissive (38°C) temperature. Wild-type (SEY6210) and *vps18^{tsf}* (SRY18T-1) spheroplasts were preincubated for 5 min at 26°C or 38°C, ^{35}S-labeled for 15 min with Expres^{35}S, and chased for 45 min at the appropriate temperature. The cultures were separated into intracellular and extracellular fractions. The vacuolar hydrolases CPY, ALP, and CPS were recovered by immunoprecipitation and visualized by SDS-PAGE and fluorography. In wild-type cells and in *vps18^{tsf}* cells at 26°C, the labeled vacuolar hydrolases were processed to their mature forms, indicative of proper delivery to the vacuole (Figure 1C, lanes 1–4). However, in *vps18^{tsf}* cells at 38°C, the vacuolar hydrolases accumulated intracellularly in their Golgi-modified precursor forms, indicating that delivery to the vacuole was blocked (Figure 1C, lanes 5 and 6). Similar results were observed for the soluble hydrolases PrA and PrB. The transport of CPY to the vacuole resumed when the *vps18^{tsf}* cells were returned to 26°C (Figure 1D). The observed recovery of CPY maturation was blocked by energy poisons but not by cycloheximide. Thus both the *vps18^{tsf}* CPY transport defect and the loss of Vps18^{tsf} protein activity were reversible. The rapid onset and ubiquitous nature of the vacuolar protein processing defects observed in *vps18^{tsf}* cells at 38°C suggest that Vps18p plays a direct role in both the CPY/CPS and ALP Golgi-to-vacuole protein transport pathways.

Although *vps18*Δ cells rapidly secrete p2CPY (Preston *et al.*, 1991; Robinson *et al.*, 1991), *vps18^{tsf}* cells accumulated the blocked p2CPY intracellularly upon shift to 38°C (Figure 1C, lanes 5 and 6), suggesting that p2CPY secretion is not an immediate consequence of loss of Vps18p function. Even after a 90-min preincubation at 38°C, the majority of the p2CPY still remained within the *vps18^{tsf}* cells. This extended intracellular retention of p2CPY was not due to a general block in protein secretion, because *vps18^{tsf}* cells at 38°C secreted multiple proteins at rates similar to wild-type cells. Furthermore, the secreted pheromone α-factor was processed normally by the late Golgi endoprotease Kex2p in *vps18^{tsf}* cells at 38°C, indicating that late Golgi function was not rapidly impaired by the loss of Vps18p function. Studies in other *vps* mutants have shown that defects in anterograde and/or retrograde transport between the late Golgi and the endosome result in the secretion of p2CPY (Marcusson *et al.*, 1994; Cereghino *et al.*, 1995; Piper *et al.*, 1995; Babst *et al.*, 1997; Cowles *et al.*, 1997; Seaman *et al.*, 1997). Thus the intracellular accumulation of p2CPY in *vps18^{tsf}* cells at 38°C suggests that Vps18p mediates a transport step distal to the endosome.

vps18^{tsf} Cells Accumulate ALP and CPS in Distinct Prevacuolar Compartments

The intracellular retention of p2CPY suggests that vacuolar precursors accumulate in transport intermediates in *vps18^{tsf}* cells at 38°C. To examine the subcellular distribution of the newly synthesized vacuolar hydrolases in *vps18^{tsf}* cells, lysates were prepared at 26°C or 38°C and subjected to differential centrifugation. Spheroplasts were ^{35}S-labeled for 15 min, chased for 45 min, and lysed. After a clearing centrifugation at 300 × *g* to remove unbroken cells, the lysate was sequentially centrifuged to generate 13,000 × *g* pellet (P13), 100,000 × *g* pellet (P100), and 100,000 × *g* supernatant (S100) fractions. When wild-type cell lysates are fractionated under these conditions (as in Figure 8), the P13 primarily contains large membrane structures, such as vacuolar membranes, plasma membrane, endoplasmic reticulum, mitochondria, and nuclei, but the P100 fraction contains Golgi membranes and transport vesicles (Marcusson *et al.*, 1994). Endosomal membranes containing the syntaxin homologue Pep12p distribute between the P13 and P100 pellets (Becherer *et al.*, 1996). Soluble proteins found in the cytosol or within the lumen of osmotically sensitive organelles are found in the S100 fraction.

The distribution of newly synthesized ALP and CPS in fractions generated from *vps18^{tsf}* cell lysates was examined by immunoprecipitation and SDS-PAGE (Figure 2A). In *vps18^{tsf}* cells at 26°C, ALP was recovered in its mature integral-membrane form in the P13 fraction, consistent with proper localization to the vac-

uole. The mature form of CPS was found in the S100 fraction, indicating that the integral-membrane CPS precursor had been processed to its soluble mature form within the lysis-sensitive vacuole. In *vps18^{tsf}* cells at 38°C, ALP was recovered in its precursor form in the P100 fraction, indicating that it was accumulating in a nonvacuolar compartment. In contrast, the CPS precursor was primarily found in a P13 fraction.

To confirm that the CPS precursor in *vps18^{tsf}* cells at 38°C was accumulating in a prevacuolar compartment as suggested by its lack of processing, equilibrium density gradient analysis of *vps18^{tsf}* cell lysates was performed (Figure 2B). An ^{35}S-labeled *vps18^{tsf}* cell lysate, prepared at 38°C as described above, was cleared at 300 × *g* and loaded on top of an Accudenz density gradient. Fractions were collected after centrifugation to equilibrium and the distribution of newly synthesized CPS was determined by immunoprecipitation and SDS-PAGE analysis. The ^{35}S-labeled CPS was found in its precursor form in the central fractions of the gradient. In contrast, Western blot analysis revealed that vacuolar membranes, defined by unlabeled mature ALP that had been properly delivered to vacuole prior to incubation at 38°C, localized to the light fractions of the gradient. A similar distribution of mature vacuolar ALP was observed in wild-type cells (see Figure 8C), indicating that the fractionation characteristics of vacuoles in *vps18^{tsf}* cells had not changed during the 38°C incubation. Thus, these subcellular fractionation experiments suggest that *vps18^{tsf}* cells accumulate the ALP and CPS precursors in distinct prevacuolar compartments.

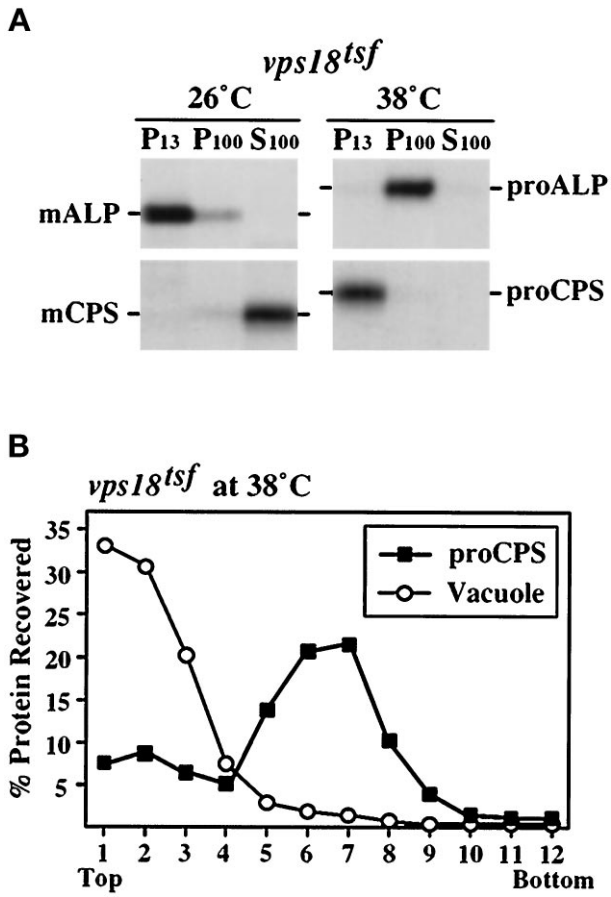

Figure 2. *vps18^{tsf}* cells accumulate ALP and CPS precursors in distinct prevacuolar compartments at 38°C. (A) Spheroplasts generated from *vps18^{tsf}* (SRY18T-1) cells were labeled for 20 min with Expres^{35}S and chased for 40 min at 26°C or 38°C before lysis in a hypotonic buffer. After centrifugation at 300 × *g*, the lysate was sequentially centrifuged to generate 13,000 × *g* pellet (P13), 100,000 × *g* pellet (P100), and 100,000 × *g* supernatant (S100) fractions. The ALP and CPS hydrolases were immunoprecipitated from each fraction, resolved by SDS-PAGE and visualized by fluorography. (B) *vps18^{tsf}* (SRY18T-1) spheroplasts were ^{35}S-labeled for 20 min and chased for 40 min 38°C, followed by lysis in a hypotonic buffer. After centrifugation at 300 × *g*, the lysate was loaded on top of an Accudenz gradient. After centrifugation to equilibrium, gradient fractions were collected, and the distribution of the labeled CPS precursors was determined by immunoprecipitation and SDS-PAGE. To localize the vacuolar membranes, the distribution of unlabeled mature vacuolar ALP was determined by Western blotting and ECL analysis.

vps18^{tsf} Cells Exhibit Defects in the Endocytic Pathway

Certain cell surface receptors, their ligands, and other plasma membrane components destined for degradation are delivered to the vacuole by the endocytic pathway, which converges with the biosynthetic pathway at a prevacuolar endosome-like compartment (Singer and Riezman, 1990; Vida *et al.*, 1993). To examine the direct consequences of the loss of Vps18p function on the endocytic pathway, *vps18^{tsf}* cells were tested for the ability to internalize and deliver endocytic markers to the vacuole at 38°C.

Bulk membrane endocytosis and vacuolar morphology were examined by staining cells with the lipophilic styryl dye FM4–64. This vital fluorescent dye initially stains the plasma membrane and then is internalized and delivered to the vacuolar membrane in a time-, energy-, and temperature-dependent manner (Vida and Emr, 1995). Wild-type and *vps18^{tsf}* cells were preincubated, stained with FM4–64, and chased in YPD at either 26°C or 38°C (Figure 3A). In wild-type cells and in *vps18^{tsf}* cells at 26°C, FM4–64 was rapidly delivered to the vacuoles that appeared as irregularly shaped brightly fluorescent compartments. In contrast, *vps18^{tsf}* cells stained at 38°C exhibited pronounced punctate staining throughout the cytoplasm and diminished vacuolar staining. The clearance of FM4–64 from the plasma membrane was not impaired in *vps18^{tsf}* cells at 38°C. The small stained compartments observed in *vps18^{tsf}* cells at 38°C may represent endocytic intermediates, as a similar punctate staining pattern is transiently observed in wild-type

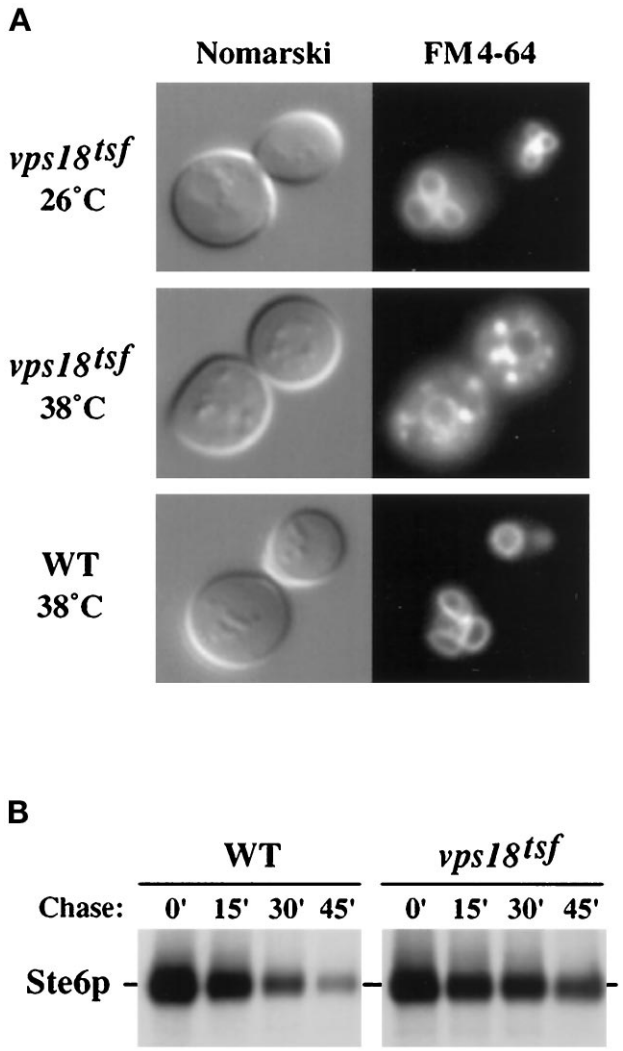

Figure 3. Endocytic transport to the vacuole in *vps18^{tsf}* mutant cells. (A) Wild-type (WT, SEY6210) and *vps18^{tsf}* (SRY18T-1) cells were stained with the vital fluorescent endocytic marker FM4–64 at 26°C or 38°C. After a chase in YPD at 26°C or 38°C, the stained cells were visualized by Nomarski (left) and fluorescence (right) microscopy. (B) The stability of the **a**-factor pheromone transporter Ste6p was determined by pulse–chase analysis. Wild-type (WT, SEY6210.1, *MAT***a**) and *vps18^{tsf}* (SRY18T-4, *MAT***a**) cells harboring pDB192 (2μ*STE6*) were grown at 26°C and shifted to 38°C for 5 min prior to labeling for 15 min at 38°C. After addition of chase (time 0′), the culture was further incubated at 38°C and samples were harvested at the time points indicated (Chase). The samples were subjected to immunoprecipitation with Ste6p-specific antiserum and analyzed by SDS-PAGE.

cells after a brief labeling with FM4–64 (Vida and Emr, 1995). Furthermore, the punctate staining in *vps18^{tsf}* cells at 38°C faded when the cells were returned to 26°C. It seems unlikely the fluorescent punctate structures represent fragmented vacuolar compartments, because 1) the vacuoles remained intact in *vps18^{tsf}* cells for several hours at 38°C (Figure 3, see Figures 4 and 5), and no defects in vacuolar segregation were observed; and 2) when the vacuoles in *vps18^{tsf}* cells were stained with FM4–64 at 26°C prior to incubation at 38°C, the punctate cytoplasmic staining was not observed. These results are most consistent with a reduction in membrane flow from endocytic intermediates to the vacuole in *vps18^{tsf}* cells at 38°C.

Endocytic traffic was analyzed further with pulse–chase experiments to monitor the delivery of Ste6p to the vacuole. Ste6p, an ABC transporter required for secretion of the **a**-factor mating pheromone, is internalized from the plasma membrane by endocytosis and delivered to the vacuole for degradation (Berkower *et al.*, 1994; Kolling and Hollenberg, 1994). To examine the degradation kinetics of Ste6p, *vps18^{tsf}* and wild-type cells harboring pDB192 (2μ*STE6*) were grown at 26°C and shifted to 38°C for 5 min prior to ^{35}S-labeling for 15 min. After the indicated chase times at 38°C, Ste6p was immunoprecipitated and analyzed by SDS-PAGE (Figure 3B). The half-life of Ste6p was increased three- to fivefold in the *vps18^{tsf}* mutant over the wild-type control. At 26°C, the stability of Ste6p was similar in *vps18^{tsf}* and wild-type cells. Earlier studies have suggested that there may be more than one degradation pathway for Ste6p (Kolling and Hollenberg, 1994), which could explain why Ste6p was not completely stabilized in *vps18^{tsf}* cells at 38°C. Because the class C *vps* null mutants are not defective in the initial internalization step of endocytosis (Dulic and Riezman, 1989, 1990), these results suggest that *vps18^{tsf}* cells accumulate both Ste6p and FM4–64 within intracellular transport intermediates instead of efficiently delivering them to the vacuole.

vps18^{tsf} Cells Exhibit Defects in the Delivery of Autophagosomes to the Vacuole

The bulk transport of cytosolic components to the yeast vacuole by autophagy is enhanced under nutrient-starvation conditions. During autophagy, cytoplasmic components are sequestered in double-membrane autophagosomes that fuse with the vacuolar membrane, resulting in the delivery of single-membrane autophagic bodies into the vacuolar lumen (Takeshige *et al.*, 1992; Baba *et al.*, 1994). In the vacuoles of wild-type cells, the autophagic bodies are rapidly degraded; however, cells lacking active vacuolar proteases show extensive accumulation of autophagic bodies within their vacuoles (Takeshige *et al.*, 1992; Baba *et al.*, 1994).

To examine whether Vps18p function is required for the delivery of autophagosomes to the vacuole, the protease-deficient strains *VPS18 pep4*Δ (TVY1) and *vps18^{tsf} pep4*Δ (SRY18–9) were incubated in nitrogen-deficient medium (SD-N) to induce autophagy. After a 2.5-h incubation at 26°C, *vps18^{tsf} pep4*Δ cells had nu-

merous autophagic bodies within their vacuoles (Figure 4A), indicating that the cytoplasmic autophagosomes were properly docking and fusing with the vacuoles. Similarly, autophagic bodies accumulated in the vacuoles of *VPS18 pep4*Δ cells at either 26°C or 38°C. In contrast, *vps18^{tsf} pep4*Δ cells at 38°C accumulated autophagosome-like compartments within the cytoplasm; furthermore, the vacuoles were devoid of autophagic bodies (Figure 4B). Most of these cytoplasmic compartments were surrounded by membrane fragments and electron-translucent RINGs, as indicated by the arrows in Figure 4B, suggesting that the autophagosomal membranes are especially sensitive to disruption during sample preparation.

Consistent with the autophagy defects observed by electron microscopy, pulse–chase analysis revealed that *vps18^{tsf}* cells exhibit a strong defect in the maturation of the vacuolar protein API at 38°C. Unlike most newly synthesized vacuolar hydrolases, API appears to be transported from the cytoplasm to the vacuolar lumen via an autophagic process (Harding *et al.*, 1996; Scott *et al.*, 1996; Schlumpberger *et al.*, 1997). Thus, these results suggest that Vps18p function is required for the docking and/or fusion of the autophagic intermediates to the vacuole.

vps18^{tsf} Cells Accumulate Small Vesicles and Clusters of Exaggerated Membrane Compartments at Nonpermissive Temperature

Class C *vps* null mutants lack morphologically recognizable vacuoles and instead accumulate small vesicles and clusters of aberrant membrane structures (Figure 5H; Banta *et al.*, 1988; Woolford *et al.*, 1990; Preston *et al.*, 1991). To investigate the morphological changes resulting directly from the inactivation of Vps18p, *vps18^{tsf}* cells were grown at 26°C, incubated for 2.5 h at 26°C or 38°C and examined by electron microscopy (Figure 5). At 26°C, *vps18^{tsf}* cells were essentially indistinguishable from wild-type cells (Figure 5A). In contrast, after a 2.5-h incubation at 38°C, a striking accumulation of membrane compartments near the vacuole was observed in *vps18^{tsf}* cells (Figure 5, B–G). Many of the accumulated structures consisted of multivesicular bodies that were reminiscent of endosomal compartments (Helenius *et al.*, 1983; Hicke *et al.*, 1997). In addition, irregularly shaped single-membrane compartments with electron-translucent content and double-membrane compartments resembling autophagosomes were observed. Such structures were not found in wild-type cells or in *vps18^{tsf}* mutant cells at 26°C. Furthermore, *vps18^{tsf}* cells at 38°C accumulated 40- to 50-nm membrane vesicles, present at levels approximately fivefold higher than observed in wild-type cells. The electron-dense vacuoles remained intact in *vps18^{tsf}* cells at 38°C, although they typically were slightly larger and more spherical than the wild-type vacuoles. The accumulation of vesicles and other membrane-enclosed compartments within *vps18^{tsf}* cells at 38°C suggests that Vps18p function may be required for the docking and/or fusion of multiple transport intermediates.

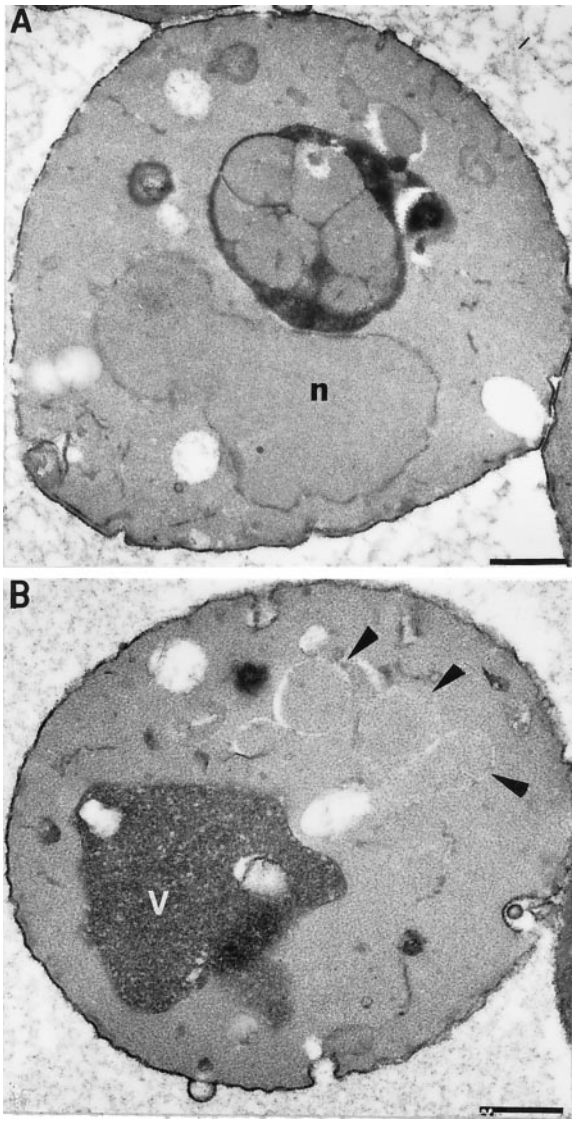

Figure 4. Examination of autophagy in *vps18^{tsf}* mutant cells by electron microscopy. *vps18^{tsf}pep4*Δ (SRY18T-9) cells were grown exponentially at 26°C and then were shifted to nitrogen-starvation medium to induce autophagy. After a 2.5-h incubation at either 26°C or 38°C, the cells were fixed and prepared for ultrastructural analysis. (A) A section of a typical *vps18^{tsf}pep4*Δ cell starved at 26°C, which contained autophagic bodies within the vacuole. (B) A section of a *vps18^{tsf}pep4*Δ cell starved at 38°C that accumulated autophagosomes in the cytoplasm (indicated by the arrows). Bars, 1 μm. The nuclei and vacuoles are labeled with the letters n and v, respectively.

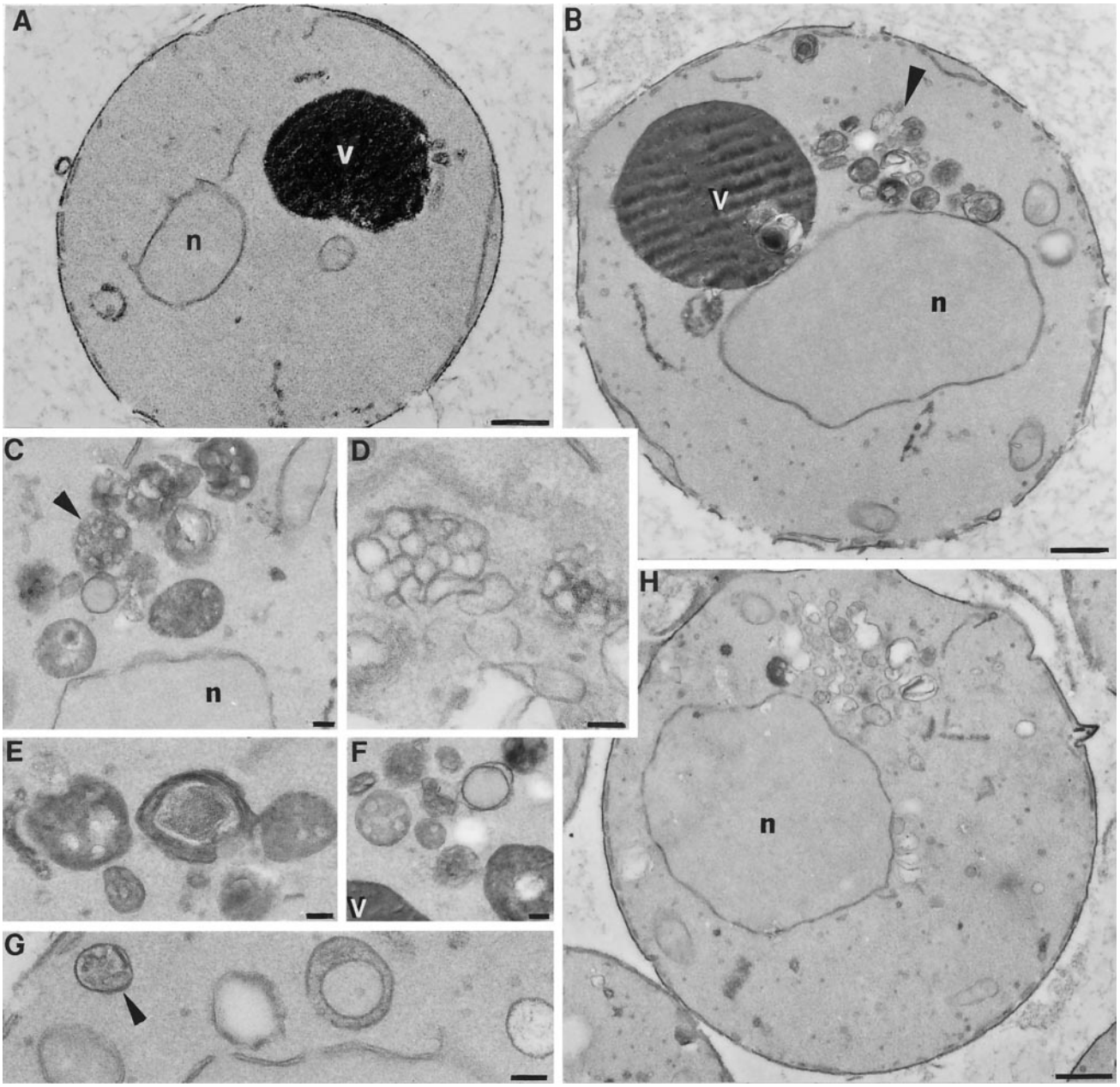

Figure 5. Ultrastructural analysis of *vps18*^{tsf} mutant cells. *vps18*^{tsf} (SRY18T-1) and *vps18-Δ1* (JSR18Δ1) cells were fixed, embedded after osmium/thiocarbohydrazide treatment and dehydration, and then sectioned and stained for electron microscopy. (A) A cross-section of a *vps18*^{tsf} (SRY18T-1) cell grown at 26°C. (B) A cell from the same culture after a 2.5-h incubation at 38°C. The arrow indicates the cluster of membrane compartments that accumulate near the vacuole in *vps18*^{tsf} cells at 38°C. (C–G) Examples of the membrane compartments in *vps18*^{tsf} cells at higher magnification. The arrows indicate some of the structures that resemble multivesicular bodies. (H) A cross-section of a *vps18-Δ1* cell (JSR18Δ1) grown at 30°C. Bars: A, B and H, 1 μm; C–G, 0.5 μm. The nuclei (n) and vacuoles (v) are labeled.

Genetic Interactions Among the Class C VPS *Genes and Other Late-acting Genes Required for Vacuolar Protein Transport*

The common phenotypes exhibited by the four class C *vps* null mutants suggests that the class C *VPS* gene products may function together to mediate a common step in protein transport to the vacuole. To explore potential genetic interactions between the class C *VPS* genes, suppression studies were conducted in the *vps18*^{tsf} strain and a *vps33* mutant strain that expresses a partially functional Vps33p (*vps33–4*; Banta *et al.*, 1990). The *vps18*^{tsf} and *vps33–4* mutant strains were

transformed with 2μ-based plasmids harboring the class C *VPS* genes, and CPY pulse–chase analyses were performed (summarized in Table 2). An ~15-fold overproduction of Vps16p suppressed the severe CPY processing defects observed in *vps18*^{tsf} cells at 36°C (Figure 6A). *vps18*^{tsf} cells harboring an empty vector matured only a small fraction of newly synthesized CPY (<5%; Figure 6A, lane 2); in contrast, *vps18*^{tsf} cells harboring the multicopy *VPS16* plasmid matured more than 70% of the newly synthesized CPY, consistent with proper transport to the vacuole (Figure 6A, lane 3). Overproduction of Vps16p also suppressed the CPY processing defects observed in *vps33–4* cells at 30°C (Figure 6B, lanes 2 and 4). In contrast, the CPY transport defects in *vps18*Δ and *vps33*Δ cells were not suppressed by overproduction of Vps16p (Table 2), indicating that excess Vps16p cannot bypass the requirement for the Vps18 or Vps33 proteins. These results and the common set of phenotypes exhibited by class C *vps* null mutants suggest that Vps18p, Vps16p, and Vps33p functionally interact to facilitate vacuolar protein transport.

The multiple transport defects observed in *vps18*^{tsf} cells at 38°C (Figures 1–5) suggest that Vps18p functions at a late step in protein transport to the vacuole. Thus potential genetic interactions between *VPS18* and other genes thought to mediate late steps in protein delivery to the vacuole were also explored. One strong candidate for interaction was *VAM3*, because it encodes a syntaxin homologue found in vacuolar membranes (Wada *et al.*, 1997). Overexpression of *VAM3* suppressed the CPY missorting phenotype of *vps18*^{tsf} mutant cells: more than 80% of the radiolabeled CPY was found as the mature species at 36°C (Figure 6A, lane 4). Overproduction of the endosomal syntaxin homologue Pep12p in *vps18*^{tsf} cells had no observable effect (Table 2). Thus, these data suggest that Vam3p and the class C Vps proteins may function in a common transport step at the vacuole.

Identification of the VPS18 and VPS11 Gene Products

To study the *VPS18* and *VPS11* gene products biochemically, polyclonal antisera were raised against TrpE-Vps18p and TrpE-Vps11p fusion proteins. The Vps18p-specific antiserum recognized a protein of 100 kDa in ^{35}S-labeled wild-type cell lysates, consistent with Vps18p's predicted molecular mass of 107 kDa, which was not isolated from *vps18*Δ cell lysates. The polyclonal antiserum raised against Vps11p recognized a protein of about 115 kDa, similar to Vps11p's predicted molecular mass of 118 kDa, which was not detected in *vps11*Δ cells. In cells carrying the *VPS18* or *VPS11* gene on multicopy 2μ-based plasmids, an ~15-fold increase in the respective gene products was observed. The abundance of Vps18p and Vps11p diminished only slightly over a 45-min chase. Both Vps18p and Vps11p appeared to constitute <0.01% of the total

Table 2. Multicopy suppression of CPY transport defect

Gene on 2μ plasmid	*vps18*^{tsf}	*vps18*Δ	*vps33-4*	*vps33*Δ
None	−	−	−	−
VPS16	+	−	+	−
VPS11	−	−	−	−
VPS18	c	c	−	−
VPS33	−	−	c	c
VAM3	+	−	−	−
PEP12	−	−	−	−

+, significant suppression; −, no suppression; c, complementation.

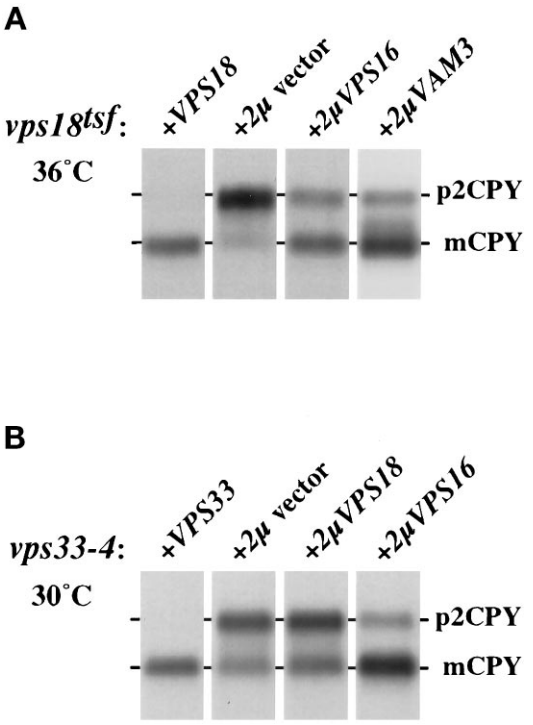

Figure 6. Genetic interactions of *VPS16*, *VPS18*, *VPS33*, and *VAM3*. (A) *vps18*^{tsf} cells (SRY18T-1) harboring various plasmids were incubated at 36°C for 5 min prior to labeling for 15 min with Expres^{35}S and chasing for 45 min at 36°C. CPY was recovered by immunoprecipitation and resolved by SDS-PAGE. The positions of Golgi-modified precursor (p2) and mature (m) CPY are indicated. The *vps18*^{tsf} cells harbored the following plasmids: vector pRS426 (2μ vector, lane 1), *CEN*-based plasmid pJSR6 (*VPS18*, lane 2), and the multicopy 2μ-based plasmids pVPS16–36 (2μ*VPS16*, lane 3) and p*VAM3*.424 (2μ*VAM3*, lane 4). (B) CPY sorting in *VPS33–4* cells harboring various plasmids was examined by pulse–chase analysis at 30°C (as described above). The following plasmids were used: vector pRS426 (2μ vector, lane 1), *CEN*-based plasmid pLB33–162 (*VPS33*, lane 2), and the multicopy 2μ-based plasmids pJR18–5 (2μ*VPS18*, lane 3) and pVPS16–36 (2μ*VPS16*, lane 4).

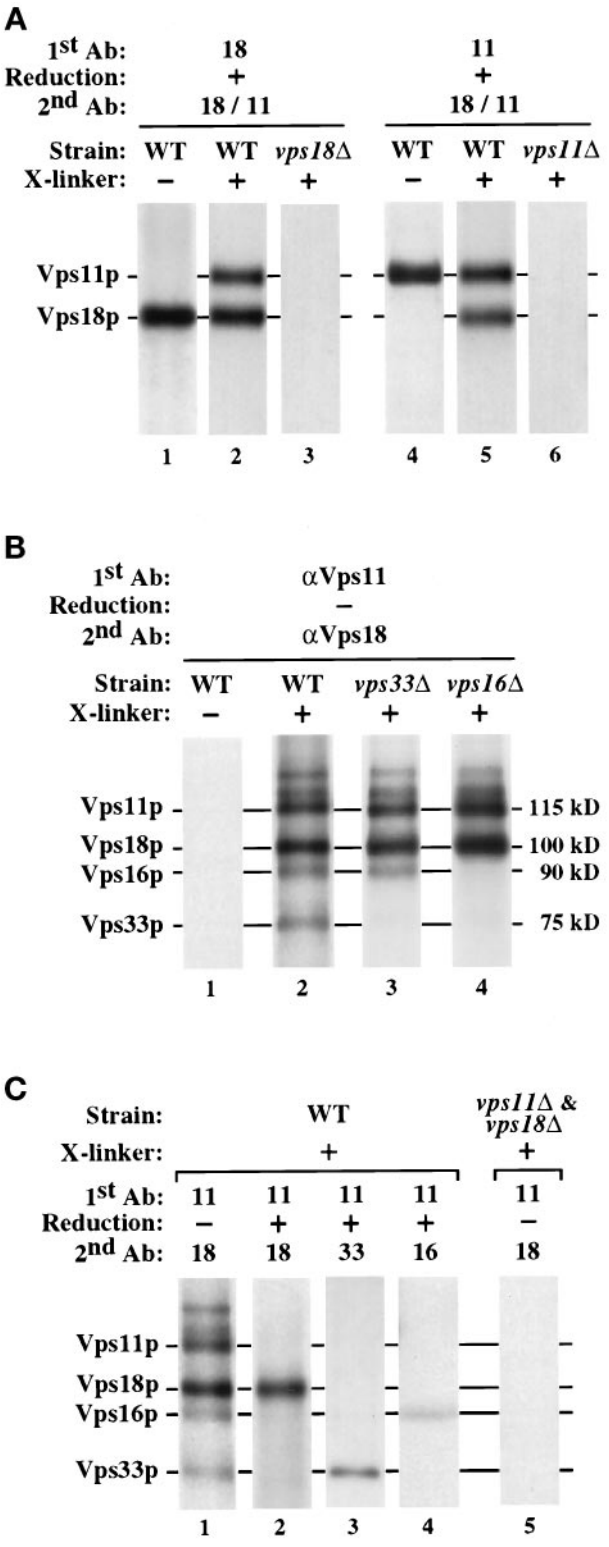

Figure 7. Class C Vps proteins physically interact in a hetero-oligomeric protein complex. (A) Spheroplasts generated from WT (wild-type, SEY6210), *vps18-Δ1* (JSR18Δ1), and *vps11-Δ2* (SEY6211*e*) strains were labeled with Expres^{35}S for 30 min, chased for 30 min, cell protein. Vps18p and Vps11p both lack recognizable signal sequences and their mobility by SDS-PAGE was unaffected by tunicamycin or endoglycosidase H treatment, indicating that these proteins do not enter the secretory pathway. Thus, these data suggest that *VPS18* and *VPS11* encode relatively rare cytoplasmic proteins.

The Class C VPS Proteins Interact in a Hetero-oligomeric Protein Complex

The shared phenotypic characteristics of the class C *vps* null mutants and the observation that *VPS18*, *VPS16*, and *VPS33* genetically interact (Figure 6) suggest that the class C Vps proteins may function together at a common step, possibly as part of a common protein complex. To determine whether the class C Vps proteins physically interact, chemical cross-linking experiments were performed using the cross-linking agent DSP. ^{35}S-labeled spheroplasts were osmotically lysed and incubated with DSP for 30 min. After quenching the cross-linking reaction, the extracts were subjected to sequential immunoprecipitations and SDS-PAGE. DSP contains a disulfide bond between its two functional reactive groups; therefore, individual components of a cross-linked complex can be resolved after treatment with a reducing agent.

In Figure 7A (lanes 1–3), DSP- and mock-treated cell extracts were subjected to immunoprecipitation with Vps18p-specific antiserum. The resulting immunoprecipitates were treated with 2-mercaptoethanol to cleave the cross-linker disulfide bond and subsequently subjected to reimmunoprecipitation

Figure 7 (cont). and then osmotically lysed. The lysates were treated with the cross-linker DSP (+ X-linker) or were mock-treated (− X-linker). The cross-linked extract was subjected to immunoprecipitation under denaturing but nonreducing conditions with Vps18p-specific antiserum (lanes 1–3) or Vps11p-specific antiserum (lanes 4–6; 1st Ab). The immunoprecipitates were reduced with 1% 2-mercaptoethanol (+ Reduction) and subjected to reimmunoprecipitation with both Vps18p- and Vps11p-specific antisera (2nd Ab). (B) Spheroplasts generated from WT (wild-type, SEY6210), *vps33-Δ2* (LBY317), and *vps16-Δ2* (BHY113) strains were ^{35}S-labeled, osmotically lysed, and treated with DSP as described above. The cross-linked and mock-treated extracts were subjected to sequential immunoprecipitations using Vps11p-specific antiserum (1st Ab) followed by reimmunoprecipitation with Vps18p-specific antiserum (2nd Ab) under denaturing, but nonreducing conditions. (C) Lanes 1–4, ^{35}S-radiolabeled WT (wild-type, SEY6210) spheroplasts were osmotically lysed and treated with DSP as described above. The cross-linked extracts were subjected to immunoprecipitation with Vps11p-specific antiserum (1st Ab). The immunoprecipitates were then treated with either reducing or nonreducing buffer (+ or − Reduction, respectively) and then reimmunoprecipitated with the indicated antisera (2nd Ab). Lane 5, ^{35}S-labeled *vps11-Δ2* (SEY6211*e*) and *vps18-Δ1* (JSR18Δ1) lysates were combined prior to treatment with DSP and subjected to sequential immunoprecipitations as described above. In all cases, the final immunoprecipitates were reduced prior to analysis by SDS-PAGE.

using both Vps11p- and Vps18p-specific antisera. Both Vps11p and Vps18p were coimmunoprecipitated with Vps18p-specific antiserum (Figure 7A, lane 2). The reciprocal experiment using Vps11p-specific antiserum first, followed by reduction and reimmunoprecipitation with both Vps11p- and Vps18p-specific antisera, also revealed a physical association between Vps11p and Vps18p (Figure 7A, lane 5). The coisolation of Vps11p and Vps18p was dependent on treatment with the cross-linker DSP (Figure 7A, lanes 1 and 4). Furthermore, neither antiserum exhibited cross-reactivity (Figure 7A, lanes 3 and 6). These results suggest that Vps18p and Vps11p associate in a hetero-oligomeric protein complex.

To determine whether other proteins could be cross-linked to Vps18p and Vps11p, experiments were performed as above, except the cross-linker was not reduced between the two immunoprecipitations. When DSP-treated lysates were subjected to sequential immunoprecipitations using Vps11p-specific antiserum followed by Vps18p-specific antiserum, a set of at least six proteins was isolated: Vps18p and Vps11p, as well as four less-abundant proteins ranging from 75 kDa to 140 kDa (Figure 7B, lane 2). Two of the proteins that associated with the cross-linked Vps18/Vps11 protein complex had apparent molecular masses similar to those of Vps16p and Vps33p (75 kDa and 90 kDa, respectively). To examine whether Vps16p and Vps33p physically interact with the Vps11/Vps18 protein complex, ^{35}S-labeled cell extracts from wild-type, *vps33*Δ and *vps16*Δ strains were treated with DSP and subjected to sequential immunoprecipitations with Vps11p- and Vps18p-specific antisera. The protein composition of the cross-linked Vps18/Vps11 protein complex was altered in the *vps33*Δ and *vps16*Δ strains: the complex from *vps33*Δ lysates lacked the 75-kDa protein, and the complex from *vps16*Δ lysates lacked both the 75-kDa and 90-kDa proteins (Figure 7B, lanes 3 and 4).

To confirm the identities of the 75-kDa and 90-kDa proteins as Vps33p and Vps16p, respectively, the cross-linked Vps18/Vps11 protein complex was isolated from ^{35}S-labeled wild-type cell lysates with Vps11p-specific antiserum, reduced, and reimmunoprecipitated with Vps18p-, Vps33p- or Vps16p-specific antiserum. As shown in Figure 7C (lanes 2–4), Vps18p, Vps33p, and Vps16p coimmunoprecipitated with Vps11p from DSP-treated cell extracts, indicating that Vps33p and Vps16p are components of the cross-linked Vps18/Vps11 protein complex. Because Vps33p is stable in *vps16*Δ cells, the loss of both Vps33p and Vps16p from the cross-linked complex in *vps16*Δ lysates (Figure 7B, lane 4) suggests that Vps16p may mediate the interaction between Vps33p and the Vps18/Vps11 protein complex. To determine whether the observed interactions between Vps11p and Vps18p were occurring before or after cell lysis, ^{35}S-labeled *vps11*Δ and *vps18*Δ cells were lysed and then combined prior to DSP treatment. It was found that the cross-linked Vps11/Vps18 protein complex did not form under these conditions (Figure 7C, lane 5).

Vps11p, Vps18p, and Vps16p Cofractionate with Vacuolar Membranes and a Distinct Dense Subcellular Fraction

To determine the potential site(s) of class C Vps protein function, subcellular fractionation studies were carried out to localize these proteins. Wild-type spheroplasts were ^{35}S-labeled for 30 min, chased for 60 min, and osmotically lysed. After a clearing centrifugation at 300 × *g*, the lysate was sequentially centrifuged at 13,000 × *g* and 100,000 × *g* to generate P13, P100, and S100 fractions. Each fraction was subjected to immunoprecipitation and SDS-PAGE analysis. Vps18p, Vps11p, and Vps16p cofractionated under these conditions (Figure 9A): the proteins were distributed between the P13 (~50%) and the P100 (~40%) fractions, with only a small fraction (<10%) residing in the S100 fraction. In contrast, Vps33p primarily behaved as a soluble protein: <10% of Vps33p was found in the P13 and P100 fractions, and the remaining 90% of Vps33p was found in the S100 fraction. The distribution of several organelle marker proteins was also determined (see Figure 9B). Vacuolar ALP was primarily recovered from the P13 fraction, and the late Golgi protein Kex2p was primarily found in the P100 fraction. As observed previously (Becherer *et al.*, 1996), the endosomal syntaxin Pep12p localized to both the P13 and P100 fractions. Neither pellet fraction was contaminated with the cytosolic enzyme glucose 6-phosphate dehydrogenase (G6PDH), indicating that little whole cell contamination or membrane aggregation occurred.

To gain further insight into the intracellular localization of the class C Vps proteins, we performed equilibrium density gradient analysis of wild-type cell lysates. An ^{35}S-labeled cell lysate was cleared at 300 × *g* and then was loaded on top of an Accudenz density gradient. After centrifugation to equilibrium, fractions were collected, and the distribution of the class C Vps proteins and the organelle markers Pep12p and mALP was determined by immunoprecipitation and SDS-PAGE. Vps18p and Vps11p cofractionated and were split between light and dense regions of the gradient. About 40% of Vps18p and Vps11p colocalized with mature vacuolar ALP, whereas the remaining 60% of Vps18p and Vps11p were found in a more dense region of the gradient (Figure 8C). Vps16p cofractionated with Vps18p and Vps11p. The portion of the class

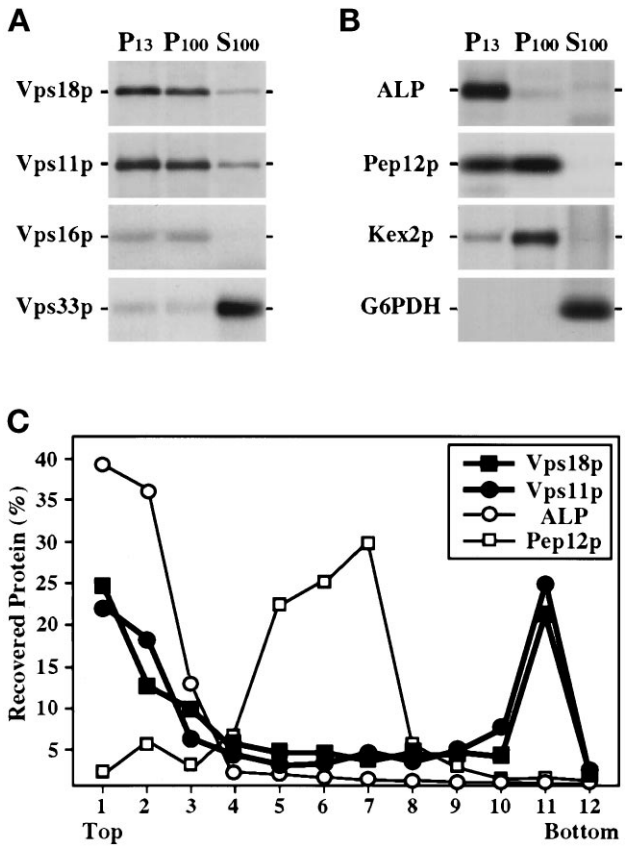

Figure 8. Subcellular localization of the class C Vps proteins. (A) Wild-type spheroplasts (SEY6210) were labeled with Expres^{35}S for 30 min and chased for 60 min before lysis in a hypotonic buffer. After centrifugation at 300 × *g*, the lysate was subjected to sequential centrifugation to generate 13,000 × *g* pellet (P13), 100,000 × *g* pellet (P100), and 100,000 × *g* supernatant (S100) fractions. The presence of Vps18p, Vps11p, Vps16p, and Vps33p in each fraction was determined by quantitative immunoprecipitation, SDS-PAGE, and fluorography. (B) The distribution of several organelle marker proteins in these fractions was also determined by immunoprecipitation: mALP (vacuole), Pep12p (endosomal compartment), Kex2p (late Golgi), and glucose 6-phosphate dehydrogenase (G6PDH, cytoplasm). (C) Accudenz gradient fractionation of cell lysates. Wild-type spheroplasts (SEY6210) were labeled for 30 min with Expres^{35}S and chased for 60 min before lysis in a hypotonic buffer. The lysate was cleared at 300 × *g* and was then loaded on top of an Accudenz gradient. After centrifugation to equilibrium, gradient fractions were collected and Vps18p, Vps11p, ALP, and Pep12p were recovered by immunoprecipitation and resolved by SDS-PAGE.

C Vps proteins found in the dense region of the gradient did not colocalize with Pep12p-containing endosomal membranes (Figure 8C) or with the late Golgi marker Vps10p. Although the plasma membrane, mitochondria, and endoplasmic reticulum also migrate to the more dense regions in similar Accudenz gradients (Singer-Kruger *et al.*, 1993), the role of the class C Vps proteins in vacuolar protein sorting makes it unlikely that they are localized to these organelles.

To examine whether the class C Vps proteins were interacting with cellular membranes, samples from the Accudenz gradient described above (Figure 8C, fractions 1–5 and 8–12) were pooled and subjected to floatation analysis. Accudenz was added to a final concentration of 40% and the samples were loaded at the bottom of Accudenz density gradients. The gradients were centrifuged to equilibrium, allowing cellular membranes to migrate from the dense load fraction into the less dense regions of the gradient due to their intrinsic buoyant densities (Zinser and Dawn, 1995). The results were similar to those observed in Figure 8C: the pool of Vps18p and Vps11p found at the top of the gradient (fractions 1–5) floated from the load fraction into the less-dense regions of the gradient with ALP, but the Vps18p and Vps11p from the dense region of the gradient (fractions 8–12) remained in the load fractions. In addition, separate floatation analyses of P13 and S13 cell fractions were performed. The pool of Vps18p and Vps11p that pelleted at 13,000 × *g* floated with ALP, but the remaining S13 pool of Vps18p and Vps11p remained in the dense Accudenz load fractions. In contrast to earlier observations (Horazdovsky and Emr, 1993), we also found that a portion of Vps16p cofractionated with vacuolar membranes. This discrepancy in the observed membrane association of Vps16p appears to be primarily due to a change in the lysis buffer, because control experiments indicated that the Tris(hydroxymethyl)aminomethane-based lysis buffer used previously destabilizes the association of the class C Vps proteins with membranes, as well as their interactions with each other. Thus, the differential centrifugation and density gradient data indicate that a significant portion of Vps18p, Vps11p, and Vps16p cofractionate with vacuolar membranes. The remaining portion of Vps18p, Vps11p, and Vps16p appears to associate with 1) a sedimentable protein complex that is not membrane-associated under these conditions or 2) an unidentified dense membrane fraction.

The Class C Vps Proteins Are Components of a Sedimentable Protein Complex

To further examine the interactions between the class C Vps proteins and pelletable cell components, cleared ^{35}S-labeled cell lysates were prepared as described above (Figure 8) and treated with various reagents prior to centrifugation at 100,000 × *g*. After mock treatment in lysis buffer, Vps18p and Vps11p were found almost exclusively in the P100 particulate cell fraction (Figure 9, lanes 1 and 2). After treatment with 1% Triton X-100, greater than 90% of Vps11p and Vps18p still pelleted at 100,000 × *g* (Figure 9, lanes 3 and 4), suggesting that they are interacting with a large protein complex. In addition, differential centrifugation experiments indicated that the portion of

Vps11p and Vps18p found in the P13 fraction in the absence of detergent (Figure 8A) shifts to the P100 fraction in the presence of Triton X-100, suggesting that this pool of Vps11p and Vps18p interacts with a sedimentable protein complex that is associated with membranes. Incubation of the cell lysates with 1 M NaCl, 2 M urea, and 0.1 M Na_2CO_3, pH 11, released the majority of Vps18p and Vps11p into the soluble S100 fraction (Figure 9, lanes 5–10), suggesting that their membrane and protein–protein associations are mediated both by ionic and hydrophobic interactions. Vps16p and the pelletable fraction of Vps33p exhibited similar solubilization characteristics as Vps18p and Vps11p. In addition, when Vps18p, Vps11p, Vps16p, or Vps33p were overproduced, most of the additional protein was found in the S100 fraction, suggesting that the association sites of these proteins with each other and/or with other sedimentable cell components was saturable. Thus, the cross-linking and subcellular fractionation data (Figures 7–9) suggest that Vps18p, Vps11p, and Vps16p, as well as a fraction of Vps33p, are components of a sedimentable protein complex and that a significant portion of the complex cofractionates with vacuolar membranes.

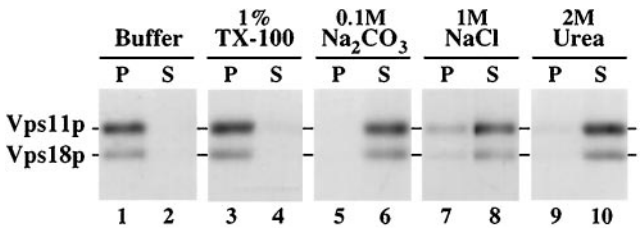

Figure 9. Class C Vps proteins are components of a sedimentable protein complex. Wild-type (SEY6210) spheroplasts were labeled for 30 min with Expres^{35}S and chased for 60 min before lysis in a hypotonic buffer. After a clearing spin at 300 × *g*, the lysates were treated with the reagents indicated for 15 min and were then centrifuged at 100,000 × *g* for 45 min to generate supernatant (S100) and pellet (P100) fractions. Vps18p and Vps11p were immunoprecipitated from each fraction, resolved by SDS-PAGE, and visualized by fluorography.

DISCUSSION

In this report, we provide complementary genetic and biochemical evidence that the class C Vps proteins (Vps18p, Vps11p, Vps16p, and Vps33p) function together in a large hetero-oligomeric protein complex to mediate the delivery of protein and membrane cargo to the vacuole. We demonstrate that the RING zinc-finger proteins Vps18p and Vps11p are components of a multiprotein complex that includes Vps16p and the Sec1p homologue Vps33p. Furthermore, we show that *VPS18*, *VPS16*, and *VPS33* genetically interact. The class C Vps protein complex appears to function at a late step in protein transport to the vacuole, because 1) the inactivation of Vps18p in *vps18^{tsf}* cells rapidly induced defects in the biosynthetic, endocytic, and autophagic pathways; 2) a substantial pool of Vps18p, Vps11p, and Vps16p colocalized with vacuolar membranes; 3) genetic interactions were observed between *VPS18* and the vacuolar syntaxin homologue *VAM3*; and 4) the inactivation of Vps18p resulted in the accumulation of morphologically distinct membrane compartments that may represent transport intermediates that are unable to dock and fuse with the vacuole. Thus, these results suggest that the class C Vps protein complex mediates the delivery of late transport intermediates to the vacuole (Figure 10).

The Class C Vps Proteins Are Components of a Novel Protein Complex

The common set of phenotypes associated with the class C *vps* mutants suggested that the class C *VPS* gene products may function at the same step in the vacuolar protein sorting pathway (Banta *et al.*, 1988; Robinson *et al.*, 1988; Raymond *et al.*, 1992). The finding that Vps18p, Vps11p, Vps16p, and Vps33p can be chemically cross-linked to each other (Figure 7) suggests that these proteins physically interact in vivo. The biological significance of these interactions is supported by the fact that the overproduction of Vps16p suppressed mutations in *VPS18* and *VPS33* (Figure 6) but did not bypass the requirement for the Vps18 or Vps33 proteins. The relative abundance of Vps16p and Vps33p in the cross-linked protein complex was lower than that of Vps18p and Vps11p (Figure 7). Although further analysis is required to examine the stoichiometry of the native class C Vps protein complex, these data suggest that Vps16p and Vps33p may associate with the Vps18/Vps11 protein complex at substoichiometric levels and thus may have regulatory functions. The finding that Vps33p failed to cross-link to Vps18p and Vps11p in *vps16*Δ mutant cells (Figure 7B), even though Vps33 protein levels were normal, suggests that Vps16p may mediate the interaction between Vps33p and the Vps18/Vps11 protein complex.

The majority of Vps18p, Vps11p, and Vps16p appear to associate with each other in a protein complex in vivo, as the three proteins cofractionated with each other during subcellular fractionation experiments (Figure 8). In contrast, only a fraction of the Vps33p within the cell appears to associate with the Vps18/Vps11/Vps16 protein complex under steady-state conditions. Less than 10% of Vps33p cofractionated with Vps18p, Vps11p, and Vps16p (Figure 8), suggesting that Vps33p may only interact transiently with the Vps18/Vps11/Vps16 protein complex. Subcellular fractionation experiments also revealed that a significant pool of Vps18p, Vps11p, Vps16p, and a small portion of Vps33p were associated with membranes yet were still sedimented at 100,000 × *g* in the presence of detergent (Figure 9). These results suggest that

the class C Vps proteins are components of a protein complex that is large enough to sediment at 100,000 × *g*; however, we cannot rule out that the possibilities that the class C Vps proteins interact with cytoskeletal elements or with membrane domains that are resistant to detergent solubilization, as observed for caveollae-associated proteins (see Parton, 1996; Harder and Simons, 1997).

Density gradient analysis indicated that ~40% of Vps18p, Vps11p, and Vps16p colocalized with mature vacuolar ALP (Figure 8C). The partial colocalization of Vps11p and Vps18p with vacuolar ALP is consistent with previous observations that the Vps11/Pep5 protein and a Vps18/Pep3-invertase fusion protein are enriched in vacuolar membrane preparations (Woolford *et al.*, 1990; Preston *et al.*, 1991). The remaining ~60% of Vps18p, Vps11p, and Vps16p localized to the dense region of the gradients (Figure 8C) and did not cofractionate with Pep12p-containing endosomal membranes nor with the Golgi. These dense fractions may contain a pool of the sedimentable class C Vps protein complex that is not associated with membranes. Alternatively, this portion of Vps18p, Vps11p, and Vps16p may interact with a very dense membrane component; possibilities include transport vesicles, a dense subdomain of vacuolar or endosomal membranes, or late transport intermediates such as "mature" endosomal compartments.

The Class C Vps Protein Complex Mediates a Late Step in Protein Transport to the Vacuole

The physical and functional interactions observed among Vps18p, Vps11p, Vps33p, and Vps16p indicate that these proteins function together in the execution of a common transport step. To examine the direct role of the class C Vps proteins, a *vps18* allele that is temperature-sensitive for function (*vps18^{tsf}*) was used to examine the immediate consequences of loss of Vps18p function on protein transport and vacuolar morphology.

Upon shift to nonpermissive temperature, *vps18^{tsf}* cells exhibited rapid defects in at least four distinct protein transport pathways to the vacuole (Figures 1–4). Newly synthesized vacuolar hydrolases transit from the late Golgi to the vacuole by at least two distinct pathways (Babst *et al.*, 1997; Cowles *et al.*, 1997). *vps18^{tsf}* cells exhibited immediate processing defects for all vacuolar hydrolases tested (including CPY, PrA, PrB, CPS, and ALP), indicating that Vps18p plays a direct role in both the ALP and CPY/CPS biosynthetic transport pathways to the vacuole. Furthermore, subcellular fractionation studies revealed that the blocked ALP and CPS precursors accumulated in distinct prevacuolar compartments in *vps18^{tsf}* cells at 38°C, suggesting that ALP and CPS transit to the vacuole in distinct transport intermediates that each require Vps18p function to deliver their cargo to the vacuole. In addition, *vps18^{tsf}* cells at 38°C exhibited defects in the delivery of endocytic markers, API, and autophagosomes to the vacuole.

The fact that inactivation of Vps18p rapidly induced defects in biosynthetic, endocytic, and autophagic traffic to the vacuole suggests that Vps18p function is required for a transport reaction common to each of these pathways. While we cannot rule out the possibility that *vps18^{tsf}* cells have a primary defect in a single transport pathway that delivers unstable components required for other transport pathways to the vacuole, this explanation seems unlikely as conditional alleles of several other *VPS* genes (i.e., *PEP12, VPS4,* and *VPS41*) do not exhibit such pleiotropic transport defects (Babst *et al.*, 1997; Cowles *et al.*, 1997). Instead, the multiple transport defects induced in *vps18^{tsf}* cells upon shift to 38°C seem to be most consistent with the class C Vps proteins having a direct role in multiple transport pathways to the vacuole.

Ultrastructural analysis revealed a striking accumulation of membrane compartments near the vacuole in *vps18^{tsf}* cells at nonpermissive temperature, suggesting that Vps18p may mediate the docking/fusion of transport intermediates to the vacuole (Figures 4 and 5). Many of the accumulated compartments consisted of multivesicular bodies reminiscent of endosomal compartments (Helenius *et al.*, 1983; Hicke *et al.*, 1997). The frequency and perivacuolar location of the aberrant structures was similar to the fluorescent staining pattern of the accumulated endocytic marker FM4–64 in *vps18^{tsf}* cells at 38°C, suggesting that at least some of these compartments may correspond to endocytic intermediates (Figures 3A and 5). Furthermore, *vps18^{tsf}* cells accumulated 40- to 50-nm membrane vesicles, 200- to 400-nm single-membrane compartments, and double-membrane compartments resembling autophagosomes (Figures 4 and 5). These compartments may represent transport intermediates from multiple pathways en route to the vacuole, which normally only transiently exist in wild-type cells. The morphology of the vacuoles in *vps18^{tsf}* cells remained essentially unaltered even after extended incubations at 38°C (Figures 3–5). Furthermore, no defects in vacuolar inheritance were observed in *vps18^{tsf}* cells at 38°C. These results indicate that Vps18p is not directly involved in maintenance of vacuolar integrity. Instead, our analysis of vacuolar protein transport and morphology in *vps18^{tsf}* cells suggests that the vacuolar morphology defects in the class C *vps* null mutants are secondary consequences due to mislocalization of vacuolar constituents required for organelle stability.

Characteristics of the Class C Vps Proteins

Vps33p is homologous to members of the Sec1 protein family, which are thought to regulate the docking of

vesicles to their appropriate target organelles (discussed further below). In contrast, the amino acid sequences and potential homologues of Vps18p, Vps11p, and Vps16p offer few direct clues to their functions; however, these proteins do have several interesting characteristics. For instance, Vps18p, Vps11p, and Vps16p have regions that are predicted to adopt α-helical coiled-coil conformations (COILS 2.1; Lupas *et al.*, 1991) and thus may contribute to protein–protein interactions (Lupas, 1996). In addition, Vps18p and Vps11p both contain C-terminal H2 RING zinc-finger domains, each of which is predicted to coordinate two zinc atoms. The RING finger zinc-binding domain and its variants are found in more than 80 proteins with diverse functions (see Borden and Freemont, 1996; Saurin *et al.*, 1996). Several of these proteins are components of membrane-associated multiprotein complexes; thus the RING finger domain may be involved in protein–protein and possibly protein–lipid interactions. For example, the mouse 43-kDa postsynaptic protein, which mediates the clustering of acetylcholine receptors at the postsynaptic membrane (Peng and Froehner, 1985; Froehner *et al.*, 1990), requires an intact H2 RING finger zinc-binding domain for its function (Scotland *et al.*, 1993). Also, the RING domain of human EEA1 contributes to the peripheral association of EEA1 with endosomal membranes in cultured cells (Stenmark *et al.*, 1996).

The integrity of the RING finger domain is important for the biological function of Vps18p, as mutation of the first conserved cysteine of the RING finger domain ($C_{826}S$) renders Vps18p temperature-sensitive for function (Figures 1–5; Robinson *et al.*, 1991). It seems unlikely that the interaction of Vps18p with Vps11p is mediated solely by the Vps18p RING finger domain, as Vps11p and the mutant Vps18 protein could still be cross-linked to each other in *vps18^{tsf}* cells at nonpermissive temperature (our unpublished results). Instead, the RING zinc-finger domains in Vps18p and Vps11p may modulate the membrane-association of the complex or mediate interactions with other proteins required for docking and fusion at the vacuole.

Interestingly, Vps18p shares significant homology with the *D. melanogaster* dor protein (BLAST p value, $7 \times e^{-28}$), a 1002-amino acid protein that contains a C-terminal H2 RING finger domain (Shestopal *et al.*, 1997). The *dor* locus was first identified in mutant flies with deep orange (dor) eyes (Stark, 1918). Most lesions in *dor* are lethal, inducing melanotic tumors and a number of other developmental defects in the larvae (see Lindsley and Zimm, 1992). Surviving *dor* mutant flies exhibit defects in pigment deposition within the eyes, ocelli, fat body, and malphighian tubules (Tearle, 1991; Lindsley and Zimm, 1992). Because pigment granules appear to be modified lysosomal compartments (Burkhardt *et al.*, 1993; Diment *et al.*, 1995; Orlow, 1995), dor is likely to be a functional homologue of Vps18p and thus may mediate the transport of multiple cargo molecules to lysosomes, including components required for pigment accumulation. Vps18p, Vps11p, and Vps16p also share significant homology with putative *Caenorhabditis elegans* proteins of unknown function and with several mammalian expressed sequence tags. Thus, it is likely that these proteins and their function in protein transport to the vacuole/lysosome are conserved throughout eukaryotic organisms.

Potential Role of the Class C Vps Proteins in Protein Transport to the Vacuole

Our results suggest that the class C Vps proteins function together in a hetero-oligomeric protein complex to mediates the delivery of late transport intermediates to the vacuole. Although our data do not reveal the precise molecular mechanisms of this process, several possibilities are consistent with our results.

Vps33p is likely to function in a manner similar to other members of the Sec1p family, which are thought to regulate the docking of vesicles to their appropriate target membranes by interacting with the appropriate syntaxin homologue at the target organelle (Hata *et al.*, 1993; Garcia *et al.*, 1994; Pevsner *et al.*, 1994; Garcia *et al.*, 1995; Hata and Sudhof, 1995). The physical and functional interactions observed between Vps33p and the other class C Vps proteins (Figures 6 and 7), as well as the genetic interactions found between *VPS18* and *VAM3* (Figure 6), suggest that Vps33p may serve as a regulatory link between the Vps18/Vps11/Vps16 protein complex and the vacuolar t-SNARE Vam3p.

It is not clear whether Sec18p is required for the transport process mediated by the class C Vps proteins and Vam3p. Previously, CPY transport studies in a temperature-conditional *sec18* strain showed that the final transport step(s) to the vacuole occurs in the absence of Sec18p activity (Graham and Emr, 1991). Recent evidence from in vitro vacuole–vacuole fusion assays indicates that Sec18p is required for a "priming" step preceding docking and fusion (Mayer *et al.*, 1996; Mayer and Wickner, 1997), such as the reactivation of SNAREs after previous docking/fusion reactions. Additional experiments will be required to resolve this apparent discrepancy and determine the precise role for Sec18p in this late transport step.

The Vps18, Vps11, and Vps16 proteins may function together as unique accessory factors required for the efficient and accurate targeting of transport intermediates to the vacuole, possibly in a manner analogous to the Exocyst complex that is required for secretion in yeast (TerBush *et al.*, 1996). Although the exact function of the Exocyst complex is not currently known, it has been proposed that the complex mediates target-

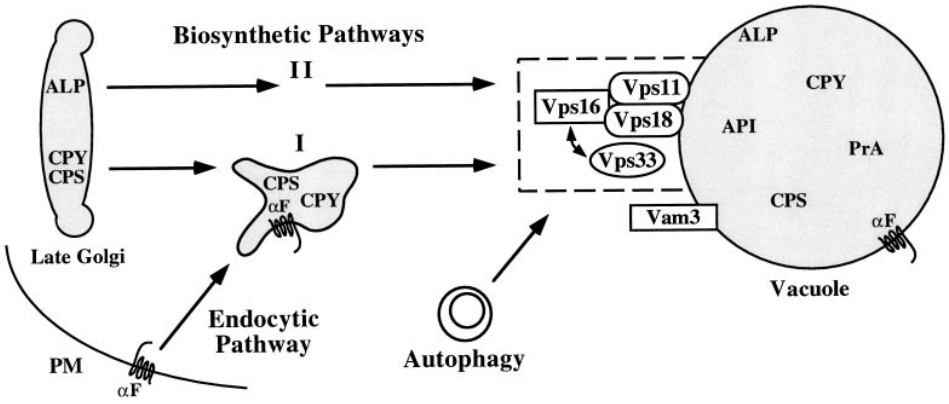

Figure 10. Class C Vps proteins mediate the delivery of multiple transport intermediates to the vacuole. The common phenotypes of the four class C *vps* null mutants, as well as the genetic interactions observed between the *VPS33*, *VPS16*, and *VPS18* genes, suggest that the class C Vps proteins function at the same transport step. Cross-linking studies indicated that Vps11p, Vps18p, and Vps16p are components of a protein complex that interacts with the Sec1p homologue Vps33p. A significant portion of the class C Vps protein complex cofractionated with vacuolar membranes. Upon shift to nonpermissive temperature, *vps18^{tsf}* cells exhibited defects in protein transport along the two distinct biosynthetic pathways (I, CPY/CPS; II, ALP), the endocytic pathway and autophagy. Furthermore, overexpression of the vacuolar syntaxin homologue Vam3p suppressed defects associated with *vps18^{tsf}* cells. Therefore, we propose that the class C Vps proteins function together with Vam3p to mediate docking and/or fusion of late transport intermediates with the vacuole.

ing of secretory vesicles to the correct docking and fusion site on the plasma membrane (TerBush *et al.*, 1996). The class C Vps protein complex shares several characteristics with the Exocyst complex. 1) The Exocyst is a large hetero-oligomeric protein complex, consisting of Sec8p, Sec15p, Sec6p, Sec5p, Sec3p, Sec10p, and Exo70p, that is required for the proper delivery of secretory vesicles to the plasma membrane (TerBush *et al.*, 1996). Similarly, our data indicate that Vps18p, Vps11p, and Vps16p physically interact in a sedimentable multiprotein complex (Figures 7–9) that mediates the targeting of transport intermediates to the vacuole (Figures 1–5). 2) Genetic interactions have been observed between the genes that encode certain components of the Exocyst complex, Sec1p, and the plasma membrane t-SNAREs (Aalto *et al.*, 1993). Similarly, genetic interactions were observed among genes encoding the class C complex members Vps18p and Vps16p, the Sec1p homologue Vps33p, and the vacuolar t-SNARE Vam3p (Figure 6). 3) The membrane-associated portion of some Exocyst components is localized to the plasma membrane at the bud tips, a major site of exocytosis (TerBush and Novick, 1995). Similarly, a substantial portion of the class C Vps protein complex colocalizes with vacuolar membranes (Figure 8), the final target of the vacuolar protein sorting pathway.

Several potential mechanisms by which the class C Vps protein complex may mediate protein transport to the vacuole can be envisioned. For example, the class C Vps proteins may form a receptor complex that contributes to appropriate docking/fusion reactions with the vacuole. Such an additional layer of regulation may be required to mediate the docking of distinct transport intermediates from the multiple pathways that converge at the vacuole. Alternatively, the class C Vps protein complex may be required for the recognition and/or formation of a subregion of the vacuole where docking and fusion occur, similar to the proposed role of the Exocyst complex at the plasma membrane. Another possibility is that the class C Vps protein complex mediates the physical contact between transport intermediates and the vacuole, either by forming a linker between the compartments or by mediating interactions between compartment membranes and cytoskeletal elements. For instance, arrays of small filaments (1–2 nm in diameter and ~5 nm long) and plaque-like areas have been observed on lysosomes and between late endosomal compartments and lysosomes in mammalian cells (Futter *et al.*, 1996). Such mechanisms could stabilize appropriate interactions between transport intermediates and the vacuole, thereby dramatically enhancing the accuracy and efficiency of protein and membrane delivery to the vacuole.

Further biochemical and genetic characterization will be required to distinguish between these and other possibilities. Future in vitro protein transport studies, along with experiments to examine physical characteristics of the class C Vps protein complex and identify other proteins that interact with the complex, should lead to further insight into the function of this novel component in protein transport to the vacuole. In addition, the purification of the multiple compartments that accumulate in *vps18^{tsf}* cells and subsequent analysis of their components will allow further characterization of the transport pathways with which they correspond. These and other studies should significantly enhance our understanding of the molecular mechanisms that regulate protein and membrane transport in yeast and other eukaryotic organisms.

ACKNOWLEDGMENTS

We are very grateful to Michael McCaffery and Tammie McQuistan for outstanding electron microscopy work at the Electron Microscopy Core B headed by Marilyn Farquhar (Program Project grant CA58689). We thank Karl Koehrer and Peggy Mustol for antibody production and Karl Koehrer for his contribution to the initial *vps18*^{tsf} vacuolar protein transport studies. David Bedwell, Robert Fuller, and Dan Klionsky are thanked for generously providing plasmids and antisera. We thank members of the Emr lab for helpful discussions and critical reading of this manuscript, especially Tamara Darsow, Christopher Burd, Erin Gaynor, and Beverley Wendland. This work was supported by grants GM-32703 and CA-58689 from the National Institutes of Health to S.D.E. S.D.E. is an Investigator of the Howard Hughes Medical Institute.

REFERENCES

Aalto, M.K., Ronne, H. and Keranen, S. (1993). Yeast syntaxins Sso1p and Sso2p belong to a family of related membrane proteins that function in vesicular transport. EMBO J. *12*, 4095–4104.

Ammerer, G., Hunter, C.P., Rothman, J.H., Saari, G.C., Valls, L.A., and Stevens, T.H. (1986). PEP4 gene of *Saccharomyces cerevisiae* encodes proteinase A, a vacuolar enzyme required for processing of vacuolar precursors. Mol. Cell. Biol. *6*, 2490–2499.

Baba, M., Takeshige, K., Baba, N., and Ohsumi, Y. (1994). Ultrastructural analysis of the autophagic process in yeast: detection of autophagosomes and their characterization. J. Cell Biol. *124*, 903–913.

Babst, M., Sato, T.K., Banta, L.M., and Emr, S.E. (1997). Endosomal transport function in yeast requires a novel AAA-type ATPase, Vps4p. EMBO J. *16*, 1820–1831.

Bankaitis, V.A., Johnson, L.M., and Emr, S.D. (1986). Isolation of yeast mutants defective in protein targeting to the vacuole. Proc. Natl. Acad. Sci. USA *83*, 9075–9079.

Banta, L.M., Robinson, J.S., Klionsky, D.J., and Emr, S.D. (1988). Organelle assembly in yeast: characterization of yeast mutants defective in vacuolar biogenesis and protein sorting. J. Cell Biol. *107*, 1369–1383.

Banta, L.M., Vida, T.A., Herman, P.K., and Emr, S.D. (1990). Characterization of yeast Vps33p, a protein required for vacuolar protein. Mol. Cell. Biol. *10*, 4638–4649.

Becherer, K.A., Rieder, S.E., Emr, S.D., and Jones, E.W. (1996). Novel syntaxin homologue, Pep12p, required for the sorting of lumenal hydrolases to the lysosome-like vacuole in yeast. Mol. Biol. Cell *7*, 579–594.

Berkower, C., Loayza, D., and Michaelis, S. (1994). Metabolic instability and constitutive endocytosis of *STE6*, the **a**-factor transporter of *Saccharomyces cerevisiae*. Mol. Biol. Cell *5*, 1185–1198.

Borden, K.L., and Freemont, P.S. (1996). The RING finger domain: a recent example of a sequence-structure family. Curr. Opin. Struct. Biol. *6*, 395–401.

Burkhardt, J.K., Wiebel, F.A., Hester, S., and Argon, Y. (1993). The giant organelles in beige and Chediak-Higashi fibroblasts are derived from late endosomes and mature lysosomes. J. Exp. Med. *178*, 1845–1856.

Cereghino, J.L., Marcusson, E.G., and Emr, S.D. (1995). The cytoplasmic tail domain of the vacuolar sorting receptor Vps10p and a subset of *VPS* gene products regulate receptor stability, function, and localization. Mol. Biol. Cell *6*, 1089–1102.

Cowles, C.R., Snyder, W.B., Burd, C.G., and Emr, S.D. (1997). An alternative Golgi to vacuole delivery pathway in yeast: identification of a sorting determinant and required transport component. EMBO J. *16*, 2769–2782.

Dieckmann, C.L., and Tzagoloff, A. (1985). Assembly of the mitochondrial membrane system. CBP6, a yeast nuclear gene necessary for synthesis of cytochrome *b*. J. Biol. Chem. *260*, 1513–1520.

Diment, S., Eidelman, M., Rodriguez, G.M., and Orlow, S.J. (1995). Lysosomal hydrolases are present in melanosomes and are elevated in melanizing cells. J. Biol. Chem. *270*, 4213–4215.

Dulic, V., and Riezman, H. (1989). Characterization of the *END1* gene required for vacuole biogenesis and gluconeogenic growth of budding yeast. EMBO J. *8*, 1349–1359.

Dulic, V., and Riezman, H. (1990). *Saccharomyces cerevisiae* mutants lacking a functional vacuole are defective for aspects of the pheromone response. J. Cell Sci. *97*, 517–525.

Dunn, W.A. (1993). Mechanism and regulation of autophagic degradation of cellular proteins. In: Advances in Cell and Molecular Biology of Membranes, Greenwich, CT: JAI Press, 117–138.

Froehner, S.C., Luetje, C.W., Scotland, P.B., and Patrick, J. (1990). The postsynaptic 43K protein clusters muscle nicotinic acetylcholine receptors in *Xenopus* oocytes. Neuron *5*, 403–410.

Futter, C.E., Pearse, A., Hewlett, L.J., and Hopkins, C.R. (1996). Multivesicular endosomes containing internalized EGF-EGF receptor complexes mature and then fuse directly with lysosomes. J. Cell Biol. *132*, 1011–1023.

Garcia, E.P., Gatti, E., Butler, M., Burton, J., and De Camilli, P. (1994). A rat brain Sec1 homologue related to Rop and UNC18 interacts with syntaxin. Proc. Natl. Acad. Sci. USA *91*, 2003–2007.

Garcia, E.P., McPherson, P.S., Chilcote, T.J., Takei, K., and De Camilli, P. (1995). rbSec1A and B colocalize with syntaxin 1 and SNAP-25 throughout the axon, but are not in a stable complex with syntaxin. J. Cell Biol. *129*, 105–120.

Graham, T.R., and Emr, S.D. (1991). Compartmental organization of Golgi-specific protein modification and vacuolar protein sorting events defined in a yeast *sec18* (NSF) mutant. J. Cell Biol. *114*, 207–218.

Gruenberg, J., and Maxfield, F. (1995). Membrane transport in the endocytic pathway. Curr. Opin. Cell Biol. *7*, 552–563.

Hanahan, D. (1983). Studies on transformation of *Escherichia coli* with plasmids. J. Mol. Biol. *166*, 557–580.

Hanson, P.I., Heuser, J.E., and Jahn, R. (1997). Neurotransmitter release—four years of SNARE complexes. Curr. Opin. Neurobiol. *7*, 310–315.

Harder, T., and Simons, K. (1997). Caveolae, DIGs, and the dynamics of sphingolipid-cholesterol microdomains. Curr. Opin. Cell Biol. *9*, 534–542.

Hata, Y., Slaughter, C.A., and Sudhof, T.C. (1993). Synaptic vesicle fusion complex contains unc-18 homologue bound to syntaxin. Nature *366*, 347–351.

Hata, Y., and Sudhof, T.C. (1995). A novel ubiquitous form of Munc-18 Interacts with multiple syntaxins. J. Biol. Chem. *270*, 13022–13028.

Hay, J.C., and Scheller, R.H. (1997). SNAREs and NSF in targeted membrane fusion. Curr. Opin. Cell Biol. *9*, 505–512.

Helenius, A., Mellman, I., Wall, D., and Hubbard, A. (1983). Endosomes. Trends Biochem. Sci. *8*, 245–250.

Herskowitz, I., and Jensen, R.E. (1991). Putting the *HO* gene to work: practical uses for mating-type switching. Methods Enzymol. *194*, 132–146.

Hicke, L., Zanolari, B., Pypaert, M., Rohrer, J., and Riezman, H. (1997). Transport through the yeast endocytic pathway occurs through morphologically distinct compartments and requires an active secretory pathway and Sec18p/*N*-ethylmaleimide-sensitive fusion protein. Mol. Biol. Cell *8*, 13–31.

Horazdovsky, B.F., DeWald, D.B., and Emr, S.D. (1995). Protein transport to the yeast vacuole. Curr. Opin. Cell Biol. *7*, 544–551.

Horazdovsky, B.F., and Emr, S.D. (1993). The *VPS16* gene product associates with a sedimentable protein complex and is essential for vacuolar protein sorting in yeast. J. Biol. Chem. *268*, 4953–4962.

Ito, H., Fukuda, Y., Murata, K., and Kimura, A. (1983). Transformation of intact yeast cells treated with alkali cations. J. Bacteriol. *153*, 163–168.

Jones, E.W. (1977). Proteinase mutants of *Saccharomyces cerevisiae*. Genetics *85*, 23–33.

Klionsky, D.J. (1997). Protein transport from the cytoplasm into the vacuole. J. Membr. Biol. *157*, 105–115.

Klionsky, D.J., and Emr, S.D. (1989). Membrane protein sorting: biosynthesis, transport and processing of yeast vacuolar alkaline phosphatase. EMBO J. *8*, 2241–2250.

Klionsky, D.J., Herman, P.K., and Emr, S.D. (1990). The fungal vacuole: composition, function, and biogenesis. Microbiol. Rev. *54*, 266–292.

Kolling, R., and Hollenberg, C.P. (1994). The ABC-transporter Ste6 accumulates in the plasma membrane in a ubiquitinated form in endocytosis mutants. EMBO J. *13*, 3261–3271.

Kornfeld, S., and Mellman, I. (1989). The biogenesis of lysosomes. Annu. Rev. Cell Biol. *5*, 483–525.

Lindsley, D.L., and Zimm, G.G. (1992). The Genome of *Drosophila melanogaster*, San Diego, CA: Academic Press.

Lupas, A. (1996). Coiled coils: new structures and new functions. Trends Biochem. Sci. *21*, 375–382.

Lupas, A., Van Dyke, M., and Stock, J. (1991). Predicting coiled coils from protein sequences. Science *252*, 1162–1164.

Maniatis, T., Fritsch, E.F., and Sambrook, J. (1982). Molecular Cloning: A Laboratory Manual, Cold Spring Harbor, NY: Cold Spring Harbor Laboratory Press.

Marcusson, E.G., Horazdovsky, B.F., Cereghino, J.L., Gharakhanian, E., and Emr, S.D. (1994). The sorting receptor for yeast vacuolar carboxypeptidase Y is encoded by the *VPS10* gene. Cell *77*, 579–586.

Mayer, A., and Wickner W. (1997). Docking of yeast vacuoles is catalyzed by the Ras-like GTPase Ypt7p after symmetric priming by Sec18p (NSF). J. Cell Biol. *136*, 307–317.

Mayer, A., Wickner W., and Haas, A. (1996). Sec18p (NSF)-driven release of Sec17p (alpha-SNAP) can precede docking and fusion of yeast vacuoles. Cell *85*, 83–94.

Miller, J. (1972). Experiments in Molecular Genetics, Cold Spring Harbor, NY: Cold Spring Harbor Laboratory Press.

Novick, P., and Zerial, M. (1997). The diversity of Rab proteins in vesicle transport. Curr. Opin. Cell Biol. *9*, 496–504.

Orlow, S.J. (1995). Melanosomes are specialized members of the lysosomal lineage of organelles. J. Invest. Dermatol. *105*, 3–7.

Parton, R.G. (1996). Caveolae and caveolins. Curr. Opin. Cell Biol. *8*, 542–548.

Peng, H.B., and Froehner, S.C. (1985). Association of the postsynaptic 43K protein with newly formed acetylcholine receptor clusters in cultured muscle cells. J. Cell Biol. *100*, 1698–1705.

Pevsner, J., Hsu, S.C., and Scheller, R.H. (1994). n-Sec1: a neural-specific syntaxin-binding protein. Proc. Natl. Acad. Sci. USA *91*, 1445–1449.

Pfeffer, S.R. (1996). Transport vesicle docking: SNAREs and associates. Annu. Rev. Cell. Dev. Biol. *12*, 441–461.

Piper, R.C., Cooper, A.A., Yang, H., and Stevens, T.H. (1995). *VPS27* controls vacuolar and endocytic traffic through a prevacuolar compartment in *Saccharomyces cerevisiae*. J. Cell Biol. *131*, 603–617.

Preston, R.A., Manolson, M.F., Becherer, K., Weidenhammer, E., Kirkpatrick, D., Wright, R., and Jones, E.W. (1991). Isolation and characterization of *PEP3*, a gene required for vacuolar biogenesis in *Saccharomyces cerevisiae*. Mol. Cell. Biol. *11*, 5801–5812.

Raymond, C.K., Howald-Stevenson, I., Vater, C.A., and Stevens, T.H. (1992). Morphological classification of the yeast vacuolar protein sorting mutants: evidence for a prevacuolar compartment in class E *vps* mutants. Mol. Biol. Cell *3*, 1389–1402.

Rieder, S.E., Banta, L.M., Kohrer, K., McCaffery, J.M., and Emr, S.D. (1996). Multilamellar endosome-like compartment accumulates in the yeast *vps28* vacuolar protein sorting mutant. Mol. Biol. Cell *7*, 985–999.

Robinson, J.S., Graham, T.R., and Emr, S.D. (1991). A putative zinc finger protein, *Saccharomyces cerevisiae* Vps18p, affects late Golgi functions required for vacuolar protein sorting and efficient alpha-factor prohormone maturation. Mol. Cell. Biol. *11*, 5813–5824.

Robinson, J.S., Klionsky, D.J., Banta, L.M., and Emr, S.D. (1988). Protein sorting in *Saccharomyces cerevisiae*: isolation of mutants defective in the delivery and processing of multiple vacuolar hydrolases. Mol. Cell. Biol. *8*, 4936–4948.

Rothman, J.E. (1994). Mechanisms of intracellular protein transport. Nature *372*, 55–63.

Rothman, J.H., Howald, I., and Stevens, T.H. (1989). Characterization of genes required for protein sorting and vacuolar function in the yeast *Saccharomyces cerevisiae*. EMBO J. *8*, 2057–2065.

Rothman, J.H., and Stevens, T.H. (1986). Protein sorting in yeast: mutants defective in vacuole biogenesis mislocalize vacuolar proteins into the late secretory pathway. Cell *47*, 1041–1051.

Rothstein, R. (1991). Targeting, disruption, replacement, and allele rescue: integrative DNA transformation in yeast. Methods Enzymol. *194*, 281–301.

Saurin, A.J., Borden, K.L., Boddy, M.N., and Freemont, P.S. (1996). Does this have a familiar RING? Trends Biochem. Sci. *21*, 208–214.

Schiestl, R.H., and Gietz, R.D. (1989). High efficiency transformation of intact yeast cells using single stranded nucleic acids as a carrier. Curr. Genet. *16*, 339–346.

Schlumpberger, M., Schaeffeler, E., Straub, M., Bredschneider, M., Wolf, D.H., and Thumm, M. (1997). *AUT1*, a gene essential for autophagocytosis in the yeast *Saccharomyces cerevisiae*. J. Bacteriol. *179*, 1068–1076.

Scotland, P.B., Colledge, M., Melnikova, I., Dai, Z., and Froehner, S.C. (1993). Clustering of the acetylcholine receptor by the 43-kD protein: involvement of the zinc finger domain. J. Cell Biol. *123*, 719–728.

Scott, S.V., Hefner-Gravink, A., Morano, K.A., Noda, T., Ohsumi, Y., and Klionsky, D.J. (1996). Cytoplasm-to-vacuole targeting and autophagy employ the same machinery to deliver proteins to the yeast vacuole. Proc. Natl. Acad. Sci. USA *93*, 12304–12308.

Seaman, M.N., Burd, C.G., and Emr, S.D. (1996). Receptor signalling and the regulation of endocytic membrane transport. Curr. Opin. Cell Biol. *8*, 549–556.

Seaman, M.N., Marcusson, E.G., Cereghino, J.L., and Emr, S.D. (1997). Endosome to Golgi retrieval of the vacuolar protein sorting receptor, Vps10p, requires the function of the *VPS29, VPS30*, and *VPS35* gene products. J. Cell Biol. *137*, 79–92.

Sherman, F., Fink, G.R., and Lawrence, L.W. (1979). Methods in Yeast Genetics: A Laboratory Manual, Cold Spring Harbor, NY: Cold Spring Harbor Laboratory Press.

Shestopal, S.A., Makunin, I.V., Belyaeva, E.S., Ashburner, M., and Zhimulev, I.F. (1997). Molecular characterization of the deep orange (*dor*) gene of *Drosophila melanogaster*. Mol. Gen. Genet. *253*, 642–648.

Sikorski, R.S., and Hieter, P. (1989). A system of shuttle vectors and yeast host strains designed for efficient manipulation of DNA in *Saccharomyces cerevisiae*. Genetics *122*, 19–27.

Singer, B., and Riezman, H. (1990). Detection of an intermediate compartment involved in transport of alpha-factor from the plasma membrane to the vacuole in yeast. J. Cell Biol. *110*, 1911–1922.

Singer-Kruger, B., Frank, R., Crausaz, F., and Riezman, H. (1993). Partial purification and characterization of early and late endosomes from yeast. Identification of four novel proteins. J. Biol. Chem. *268*, 14376–14386.

Spormann, D.O., Heim, J., and Wolf, D.H. (1991). Carboxypeptidase yscS: gene structure and function of the vacuolar enzyme. Eur. J. Biochem. *197*, 399–405.

Stack, J.H., Horazdovsky, B., and Emr, S.D. (1995). Receptor-mediated protein sorting to the vacuole in yeast. Annu. Rev. Cell. Dev. Biol. *11*, 1–33.

Stark, M.B. (1918). A hereditary tumor in the fruit fly, *Drosophila*. J. Cancer Res. *3*, 279–301.

Stenmark, H., Aasland, R., Toh, B.H., and D'Arrigo, A. (1996). Endosomal localization of the autoantigen EEA1 is mediated by a zinc-binding FYVE finger. J. Biol. Chem. *271*, 24048–24054.

Takeshige, K., Baba, M., Tsuboi, S., Noda, T., and Ohsumi, Y. (1992). Autophagy in yeast demonstrated with proteinase-deficient mutants and conditions for its induction. J. Cell Biol. *119*, 301–311.

Tearle, R. (1991). Tissue specific effects of ommochrome pathway mutations in *Drosophila melanogaster*. Genet. Res. *57*, 257–266.

TerBush, D.R., Maurice, T., Roth, D., and Novick, P. (1996). The Exocyst is a multiprotein complex required for exocytosis in *Saccharomyces cerevisiae*. EMBO J. *15*, 6483–6494.

TerBush, D.R., and Novick, P. (1995). Sec6, Sec8, and Sec15 are components of a multisubunit complex which localizes to small bud tips in *Saccharomyces cerevisiae*. J. Cell Biol. *130*, 299–312.

Traub, L.M., and Kornfeld, S. (1997). The *trans*-Golgi network: a late secretory sorting station. Curr. Opin. Cell Biol. *9*, 527–533.

Vida, T.A., and Emr, S.D. (1995). A new vital stain for visualizing vacuolar membrane dynamics and endocytosis in yeast. J. Cell Biol. *128*, 779–792.

Vida, T.A., Huyer, G., and Emr, S.D. (1993). Yeast vacuolar proenzymes are sorted in the late Golgi complex and transported to the vacuole via a prevacuolar endosome-like compartment. J. Cell Biol. *121*, 1245–1256.

Wada, Y., Kitamoto, K., Kanbe, T., Tanaka, K., and Anraku, Y. (1990). The *SLP1* gene of *Saccharomyces cerevisiae* is essential for vacuolar morphogenesis and function. Mol. Cell Biol. *10*, 2214–2223.

Wada, Y., Nakamura, N., Ohsumi, Y., and Hirata, A. (1997). Vam3p, a new member of syntaxin related proteins, is required for vacuolar assembly in the yeast *Saccharomyces cerevisiae*. J. Cell Sci. *110*, 1299–1306.

Wada, Y., Ohsumi, Y., and Anraku, Y. (1992). Genes for directing vacuolar morphogenesis in *Saccharomyces cerevisiae*. J. Biol. Chem. *267*, 18665–18670.

Woolford, C.A., Dixon, C.K., Manolson, M.F., Wright, R., and Jones, E.W. (1990). Isolation and characterization of *PEP5*, a gene essential for vacuolar biogenesis in *Saccharomyces cerevisiae*. Genetics *125*, 739–752.

Zinser, E., and Daum, G. (1995). Isolation and biochemical characterization of organelles from the yeast, *Saccharomyces cerevisiae*. Yeast *11*, 493–536.